San Jose State University

SJSU ScholarWorks

1-1-2022

Eocene dike orientations across the Washington Cascades in response to a major strike-slip faulting episode and ridge-trench interaction

Robert B. Miller
San Jose State University, robert.b.miller@sjsu.edu

Kathleen I. Bryant
San Jose State University

Brigid Doran
San Jose State University

Michael P. Eddy
College of Science

Franco P. Raviola
San Jose State University

See next page for additional authors

Follow this and additional works at: https://scholarworks.sjsu.edu/faculty_rsca

Recommended Citation

Authors

Robert B. Miller, Kathleen I. Bryant, Brigid Doran, Michael P. Eddy, Franco P. Raviola, Nicholas Sylva, and Paul J. Umhoefer

Eocene dike orientations across the Washington Cascades in response to a major strike-slip faulting episode and ridge-trench interaction

Robert B. Miller[1], Kathleen I. Bryant[1], Brigid Doran[1], Michael P. Eddy[2], Franco P. Raviola[1], Nicholas Sylva[1], and Paul J. Umhoefer[3]

[1]Department of Geology, San Jose State University, San Jose, California 95192-0102, USA
[2]Department of Earth, Atmospheric, and Planetary Sciences, Purdue University, West Lafayette, Indiana 47907, USA
[3]School of Earth and Sustainability, Northern Arizona University, Flagstaff, Arizona 86011, USA

ABSTRACT

The northern Cascade Mountains in Washington (USA) preserve an exceptional shallow to mid-crustal record of Eocene transtension marked by dextral strike-slip faulting, intrusion of dike swarms and plutons, rapid non-marine sedimentation, and ductile flow and rapid cooling in parts of the North Cascades crystalline core. Transtension occurred during ridge-trench interaction with the formation of a slab window, and slab rollback and break-off occurred shortly after collision of the Siletzia oceanic plateau at ca. 50 Ma. Dike swarms intruded a ≥1250 km² region between ca. 49.3 Ma and 44.9 Ma, and orientations of more than 1500 measured dikes coupled with geochronologic data provide important snapshots of the regional strain field. The mafic Teanaway dikes are the southernmost and most voluminous of the swarms. They strike NE (mean = 036°) and average ~15 m in thickness. To the north, rhyolitic to basaltic dikes overlap spatially with 49.3–46.5 Ma, mainly granodioritic plutons, but they typically predate the nearby plutons by ca. 500 k.y. The average orientations of five of the six dike domains range from 010° to 058°; W-NW– to NW–striking dikes characterize one domain and are found in lesser amounts in a few other domains. Overall, the mean strike for all Eocene dikes is 035°, and the average extension direction (305°–125°) is oblique to the strike (~320°) of the North Cascades orogen. Extension by diking reached ~45% in one >7-km-long transect through the Teanaway swarm and ranged from ~5% to locally ~79% in shorter transects across other swarms, which corresponds to a minimum of ~12 km of extension.

The dominant NE-striking dikes are compatible with the dextral motion on the N- to NW-striking (~355–320°) regional strike-slip faults. Some of the W–NW- to NW-striking dikes were arguably influenced by pre-existing faults, shear fractures, and foliations, and potentially in one swarm where both NE- and lesser W-NW–striking dikes are present, by a switch in principal stress axes induced by dike emplacement. Alternatively, the W-NW– to NW-striking dikes may reflect a younger regional strain field, as ca. 49.3–47.5 Ma U-Pb zircon ages of the NE-striking dikes are older than those of the few dated W-NW– to NW-trending dikes. In one scenario, NE-striking dikes intruded during an interval when strain mainly reflected dextral strike-slip faulting, and the younger dikes record a switch to more arc-normal extension. Diking ended as magmatism migrated into a N-S–trending belt west of the North Cascades core that marks the initiation of the ancestral Cascade arc.

■ INTRODUCTION

Ridge-trench interaction and related slab window formation or slab break-off is hypothesized to result in anomalous magmatism and changes in the regional stress regime in the overriding plate (e.g., Dickinson and Snyder, 1979; Thorkelson and Taylor, 1989; Thorkelson, 1996; Sisson et al., 2003). The U.S. Pacific Northwest and southwestern British Columbia (Canada) are postulated to have been a site of slab window formation and slab breakoff at ca. 50–45 Ma, when the Farallon—Kula or Farallon—Resurrection spreading ridge interacted with the North American plate (Fig. 1) (e.g., Breitsprecher et al., 2003; Haeussler et al., 2003a; Madsen et al., 2006; Eddy et al., 2016a; Kant et al., 2018). Thick oceanic crust formed along this ridge in a setting that is likely analogous to that of modern Iceland, as indicated by Siletzia, which is a large igneous province associated with the ridge (e.g., Wells et al., 2014). This terrane accreted to North America, from southwestern Oregon to southern Vancouver Island, between ca. 53 Ma and 49 Ma (McCrory and Wilson, 2013; Wells et al., 2014; Eddy et al., 2016a, 2017a, 2017b), and the spreading ridge likely underthrust the continent near southern to central Vancouver Island (Fig. 1) as indicated by 51–49 Ma near-trench intrusions (Groome et al., 2003; Madsen et al., 2006) and the 51–50 Ma, partially ophiolitic Bremerton and Metchosin complexes (Massey, 1986; Clark, 1989; Eddy et al., 2017a).

The arrival of the ridge and Siletzia at the trench strongly influenced Eocene deformation and is inferred to have resulted in brief (<3 m.y.) crustal shortening (Johnston and Acton, 2003; Wells et al., 2014; Eddy et al., 2016a; 2017b; Miller et al., 2016; Gundersen, 2017). Initiation and/or increased movement of dextral

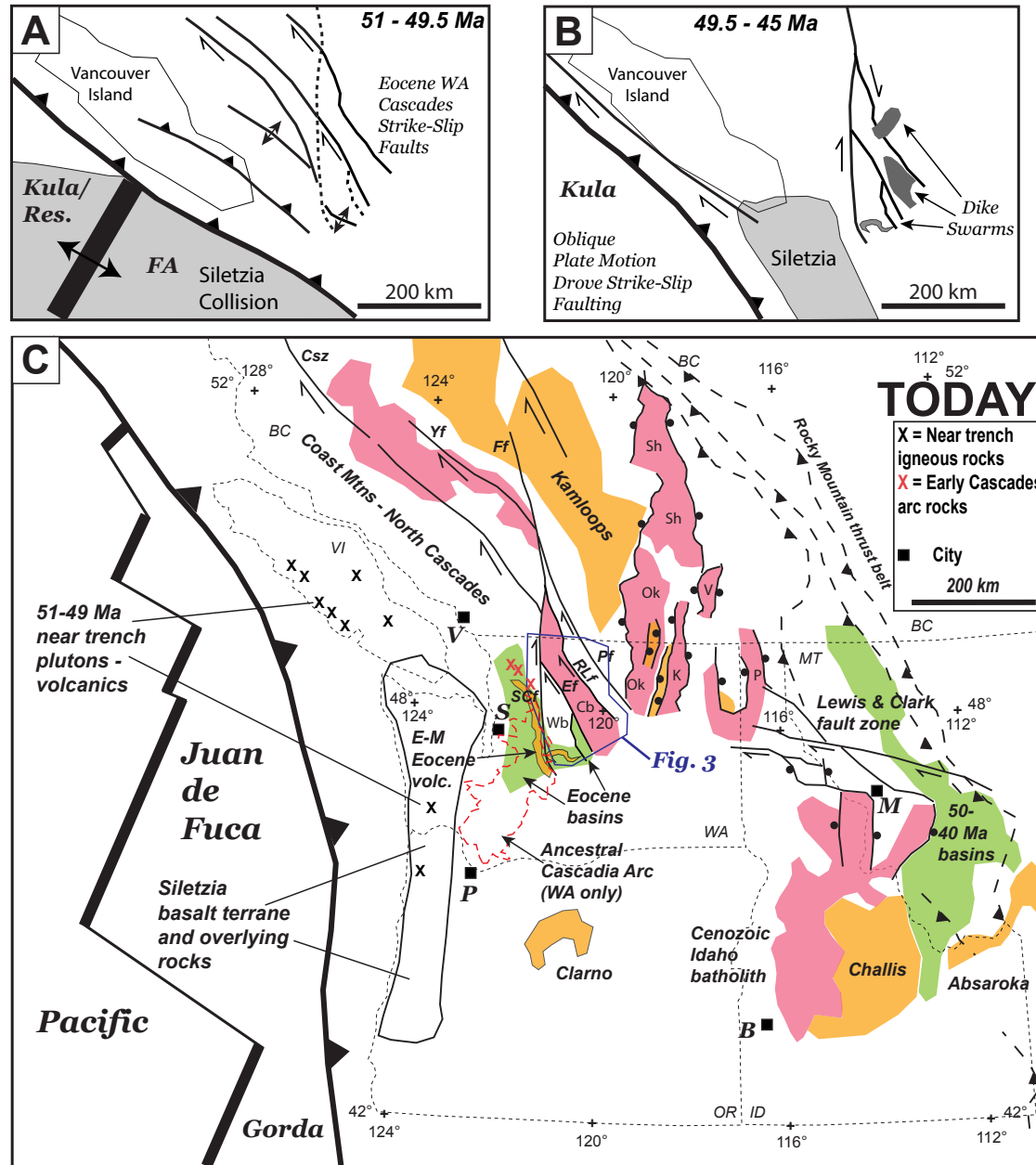Robert Miller https://orcid.org/0000-0002-2006-4963

Figure 1. (A) Tectonic map illustrates probable Paleogene ridge-trench interaction and collision of Siletzia in northwestern United States and southwestern British Columbia at 51–49.5 Ma. The fold and thrust belt resulting from collision and active dextral strike-slip faults in the Cascades are shown. The dashes and the northeastern strike-slip fault are the boundaries of the crystalline core of the North Cascades. Vancouver Island has been restored to its position prior to ca. 150 km of dextral slip on the Straight Creek-Fraser River fault (see text). FA—Farallon plate; Res.—Resurrection plate. WA—Washington. Modified from Eddy et al. (2017b). (B) Tectonic map after Siletzia collision emphasizes the location of the dike swarms described in this paper and the active dextral strike-slip faults in the Cascades. (C) Simplified map of U.S. Pacific Northwest and southern British Columbia emphasizes early Cenozoic tectonic features. Many of these features overlapped temporally with dike swarms, whereas the Early Cascades arc rocks and Ancestral Cascade arc formed nearly directly after diking ended. Orange—Eocene volcanic rocks; pink—crystalline rocks of Paleogene age or ductilely deformed in the Paleogene; green—Paleogene basins. Ball on downthrown sides of faults bounds metamorphic core complexes. Cb—Chelan block of North Cascades crystalline core; Csz—Coast shear zone; Ef—Entiat fault; Ff—Fraser fault; K—Kettle core complex; Ok—Okanogan core complex; P—Priest River core complex; Pf—Pasayten fault; RLf—Ross Lake fault; SCf—Straight Creek fault; Sh—Shuswap core complex; V—Valhalla complex; Wb—Wenatchee block of North Cascades crystalline core; Yf—Yalakom fault. Blue polygon shows location of Figure 3. Cities: B—Boise; M—Missoula; P—Portland; S—Seattle; V—Vancouver. E-M—Eocene-Miocene.

strike-slip faults in Washington and southern British Columbia occurred during and after collision at 50–49 Ma and was coincident with juxtaposition of this part of the North American margin with the Kula or Resurrection plate (Eddy et al., 2016a). Rollback and break-off of the Farallon slab as a result of Siletzia collision (Schmandt and Humphreys, 2011) induced vigorous magmatism in the northern Washington Cascades from ca. 49.3 Ma to 45 Ma (Eddy et al., 2016a; Miller et al., 2016; Kant et al., 2018). A new subduction zone formed outboard of Siletzia and initiated the N-S–trending ancestral Cascade arc at ca. 45–44 Ma (Schmandt and Humphreys, 2011; Kant et al., 2018).

Variable exhumation exposed mid- and upper-crustal rocks in the central and northern Washington Cascades, which provide a record of both ductile and brittle Eocene deformation (Miller et al., 2016). This transtensional deformation includes ductile subhorizontal stretching in the crystalline core of the North Cascades (Cascades core), dextral strike-slip and dextral-normal oblique faulting, intrusion of dike swarms in and adjacent to the Cascades core, and

rapid basin subsidence and sediment accumulation in the upper crust (e.g., Haugerud et al., 1991a; Eddy et al., 2016a; Miller et al., 2016). Large, dominantly granodioritic plutons intruded the northern part of the Cascades core between ca. 49.3 Ma and 45.5 Ma and overlapped in age with dike emplacement. The dike swarms extensively intruded a ≥1250 km^2 region of the central and northern Washington Cascades over an interval of <5 m.y. and make up ~30% to ≥60% of the rock in some tens of square kilometer areas. These Eocene dikes are the focus of this study.

Dikes are useful for understanding the stress and strain at the time of their intrusion into a homogeneous isotropic material, as they strike perpendicular to the least compressive stress (σ_3) and should be subvertical in the shallow crust (Anderson, 1951). Dike orientations are thus commonly interpreted to record the regional stress and strain field (Fig. 2) (e.g., Zoback and Zoback, 1980; Ernst et al., 1995; Haeussler et al., 2003b), but trends may be modified by mechanical anisotropy (e.g., Jourdan et al., 2006; Gudmundsson, 2011;
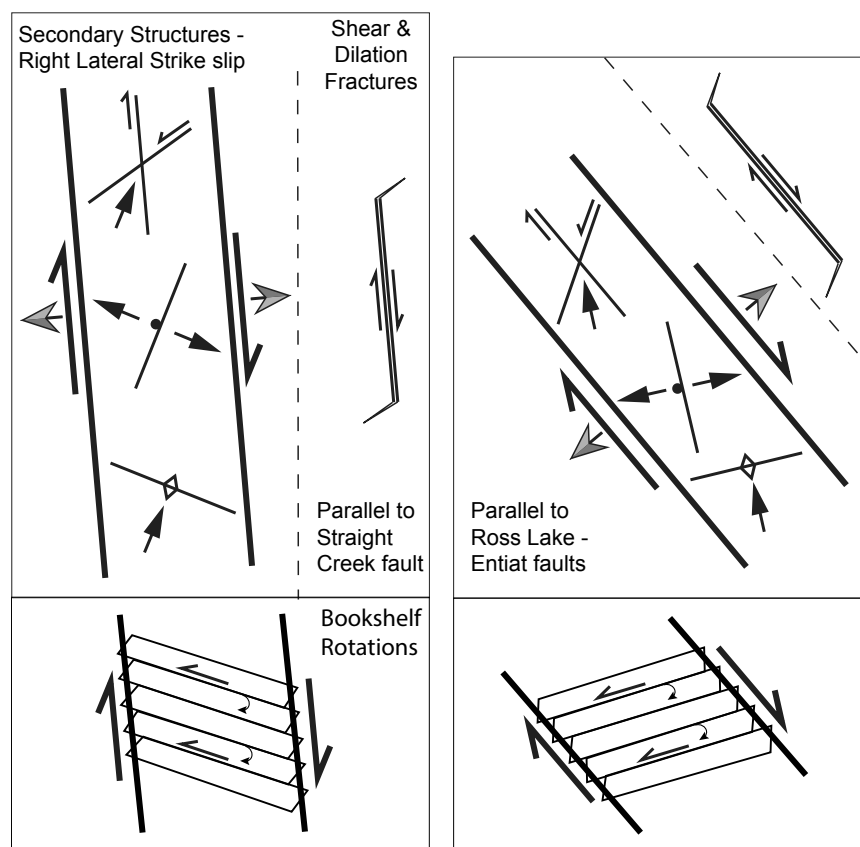

Figure 2. Diagrams show potential orientations of secondary structures associated with right-lateral strike-slip faults during transtension. Left panels are for the Straight Creek fault (350–355° strike), and right panels are for the Ross Lake and Entiat faults (strike ~315–320°). Secondary structures include conjugate strike-slip faults (R and R′ orientations), folds, dikes-normal faults (same orientation), and folds. Orientations of shear and dilation fractures are also shown. Angles between dikes and major faults will be lower in efficiently partitioned transtension. "Bookshelf rotations" illustrate the potential for development of sinistral faults and clockwise rotations.

Martínez-Posa et al., 2014; Gans and Gentry, 2016; Wadge et al., 2016), magma pressure (e.g., Muller and Pollard, 1977; Delaney et al., 1986; Parsons and Thompson, 1991), and tectonic rotation (e.g., Wells et al., 2014). Dikes may also open obliquely during transtension (e.g., Delaney et al., 1986; Glazner et al., 1999). The thickness of a dike is commonly interpreted to record the amount of magmatic dilation or elongation (typically referred to as extension, as in this study) accommodated by its emplacement.

Dike orientations and thicknesses, in conjunction with other structural data, may thus provide important information about the direction and magnitude of extension. We use such an approach by reporting the orientations of more than 1500 dikes to evaluate the regional strain field of the North Cascades of Washington at ca. 50–45 Ma during ridge-trench interaction and transtension. The influence of structural anisotropy and magma pressure on dike orientations, and potential subsequent tectonic rotations, are also examined. Many regional dike studies are done on large igneous provinces associated with rifting (e.g., Iceland, East Africa), and relatively few regional studies of this type have been conducted in the western North America Cordillera, and this is particularly true for a major transtensional belt (e.g., Wolf and Saleeby, 1992; Glazner et al., 1999; Bartley et al., 2007). Our work compliments studies on slightly older dikes in southern Alaska, which are also inferred to have intruded during ridge-trench interaction (Haeussler et al., 2003b).

Geologic Setting

The North Cascades consists of a crystalline core of metamorphic rocks and Cretaceous to Paleogene plutons, which are juxtaposed against lower-grade to non-metamorphic Paleozoic and Mesozoic rocks and Paleogene clastic strata (Fig. 3) (Misch, 1966; Brown, 1987). The North Cascades experienced mid-Cretaceous (ca. 90 Ma) shortening, crustal thickening, and Barrovian metamorphism followed by regional transpression from ca. 73 Ma to 55 Ma (e.g., Misch, 1966; Miller and Bowring, 1990; McGroder, 1991; Paterson et al., 2004). Ensuing transtension lasted until at least 45 Ma (Haugerud et al., 1991a; Miller et al., 2016).

Major Eocene high-angle faults (Fig. 3) formed during transtension and include the Straight Creek-Fraser River fault and Ross Lake fault zones, which bound the Cascades core on the west and northeast, respectively (Misch, 1966). Estimates of dextral strike slip on the Straight Creek fault range from 90 km to 190 km (Misch, 1977a; Vance and Miller, 1983; Tabor et al., 1984; Monger, 1986; Umhoefer and Miller, 1996), and the most recent estimate favors ~150 km (Monger and Brown, 2016). The Ross Lake fault zone experienced early (≥65 Ma to ca. 57 Ma) dextral-reverse motion followed by dextral-normal slip that lasted until ca. 49–48 Ma in the south and perhaps 45 Ma in the north (Miller and Bowring, 1990; Haugerud et al., 1991a). The Straight Creek-Fraser River fault truncates the Ross Lake fault zone and probably initiated by 49 Ma and ended before 34 Ma (e.g., Tabor et al., 1984; Monger, 1986). The Entiat fault and Leavenworth fault zone are the other major Eocene high-angle faults and

place the Cascades core against Paleogene sedimentary rocks (Fig. 3). These faults had both dextral and vertical motion (Gresens et al., 1981; Evans, 1994; Cheney and Hayman, 2009; Eddy et al., 2017b). The Entiat fault also cuts into the crystalline core, where it separates the Wenatchee block on the SW—which lacks Eocene magmatism and typically has K-Ar and Ar/Ar biotite cooling ages of >60 Ma—from the Chelan block on the NE, which was intruded by Eocene plutons and has mostly younger cooling ages (Tabor et al., 1989).

Non-marine sedimentary basins formed before and during transtension include the greater Swauk basin (Fig. 3), which accumulated sediments from ≤59 Ma to ca. 51 Ma (Eddy et al., 2016a). This basin experienced a short-lived episode of folding that is attributed to the collision of Siletzia, which was followed at ca. 49.3 Ma by eruption of dominantly basaltic lavas of the Teanaway Formation (e.g., Tabor et al., 1984; Eddy et al., 2016a). This volcanism was close in age to initiation of the strike-slip Chumstick basin (Eddy et al., 2016a; Donaghy et al., 2021), which continued receiving sediment until ca. 44 Ma and is separated from the Swauk and Cascades core rocks on the SW by the Leavenworth fault and from Cascades core rocks on the NE by the Entiat fault (Fig. 3).

Intrusion of mafic to felsic dikes occurred from at least 49.3 Ma to 44.9 Ma in a region that covers a minimum of 150 km in a N-S direction; dikes are discontinuously exposed in concentrated areas within that region (Fig. 3). The basaltic Teanaway dikes represent a high-volume dike swarm that intrudes the Swauk basin at the southern end of the region of diking, whereas dikes to the north are more variable in local volumes and composition and include granite porphyries, rhyolites, andesites, and basalts (e.g., Misch, 1977b; Tabor et al., 1987). Dikes north of the Teanaway swarm intrude the Chelan block of the Cascades core and the Jura-Cretaceous Methow basin. Some of these dikes are associated spatially with dominantly granodioritic Eocene plutons (Fig. 3). Eocene dikes only locally intrude the Wenatchee block of the core.

Eocene dikes, dextral faults, basins, and ductile structures in the Cascades are broadly coeval with Eocene metamorphic core complexes, volcanic and plutonic rocks, dikes, and fault-bounded, N- to N-NE–trending non-marine basins in northeast Washington and southern British Columbia (Fig. 1C) (e.g., Ewing, 1980; Parrish et al., 1988; Eddy et al., 2016a; Miller et al., 2016). Dikes in this region are not well dated, but most K-Ar dates from volcanic rocks in the basins range between 51 Ma and 48 Ma (Pearson and Obradovich, 1977), and thus the volcanic rocks overlap temporally with the older (49–48 Ma) dikes in the Cascades. Sediments were deposited in the basins in the region from ca. 54–48 Ma (Pearson and Obradovich, 1977; Suydam and Gaylord, 1997). Similarly, the youngest mylonites in the Okanogan Complex, the core complex closest to the North Cascades, formed between ca. 50 Ma and 49 Ma (Parrish et al., 1988; Kruckenberg et al., 2008).

In this report, we focus on orientations, abundances, and thicknesses of Eocene dikes that intrude the northern Washington Cascades (Fig. 3). Emphasis is placed on the Teanaway dike swarm, which is the most voluminous and best-studied swarm. Other Eocene dikes studied in detail are, from south to north: the Corbaley Canyon swarm, dikes near the southern end of the Eocene Duncan Hill pluton, dikes near the eastern margin of the Duncan Hill pluton,
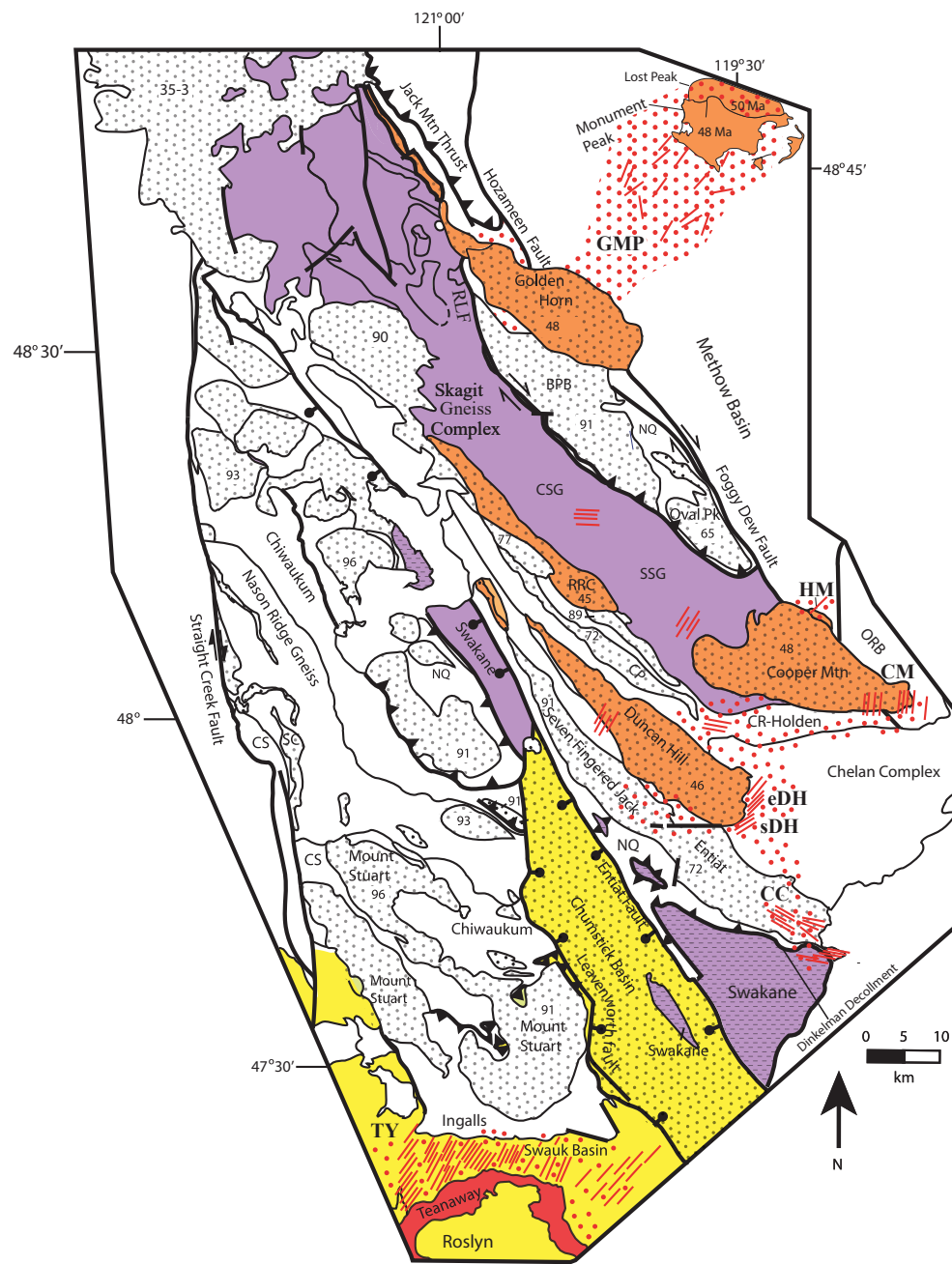
Figure 3. Map of the North Cascades emphasizes Eocene dikes, plutons, and volcanic rocks. Much of the area is in the Cascades core, which is composed of the crystalline rocks between the Straight Creek fault on the west and the Ross Lake and Foggy Dew fault zones on the east. The red dotted pattern indicates areas with abundant Eocene dikes, and red lines are representative dike strikes. Dike domains (in bold) discussed in this manuscript include the Corbaley Canyon (CC), Cooper Mountain (CM), eastern Duncan Hill (eDH), Golden Horn-Monument Peak (GMP), Hungry Mountain (HM), southern Duncan Hill (sDH), and Teanaway (TY) domains. Numbers in plutons are inferred crystallization ages, and Eocene plutons are in orange. The Skagit Gneiss Complex and Swakane Gneiss (both shown in purple) have Eocene Ar/Ar biotite cooling ages. Other names include the Black Peak batholith (BPB), Cardinal Peak pluton (CP), Chiwaukum Schist (CS), central Skagit Gneiss (CSG), Cascade River-Holden-Twentyfive Mile Creek Schist (CR-Holden), Napeequa unit (NQ), Okanogan Range batholith (ORB), Railroad Creek pluton (RRC), and southern Skagit Gneiss Complex (SSG). SC—Sloan Creek plutons; RLF—Ross Lake fault.

dikes near the Eocene Cooper Mountain batholith, and dikes near the Eocene Golden Horn batholith and Monument Peak stock (Fig. 3). We also briefly report on less well-studied and well-dated dikes that intrude the Cascades core N and NW of the Duncan Hill and Cooper Mountain plutons (Fig. 3). Using these data and our U-Pb dates of dikes, we focus on the controls of dike orientations. In particular, we evaluate the regional strain field and the influence of structural anisotropies and magma centers that are broadly coeval with the dikes. The magnitudes of extension from diking are also estimated for some of the swarms. Finally, we synthesize these data and their implications for regional transtension and ridge-trench interaction.

Field Methods

Dike composition, orientation, and thickness were determined for most of the dikes from the study areas. Exceptions for thickness included dikes with only one wall exposed. Orientations where the two dike walls are not parallel, but are within 20°, were averaged.

Orientations of dikes were measured as part of mapping and structural analysis concentrating on metamorphic and plutonic rocks in the North Cascades (e.g., Cooper Mountain and western Golden Horn dikes; Raviola, 1988) and as more focused studies of dikes (Teanaway, Corbaley Canyon, and Duncan Hill dikes; Doran, 2009; Bryant, 2017). Dike strikes were also summarized from other workers (Tabor et al., 1968; Mendoza, 2008). Thus, the level of detail and uncertainties varied among different domains.

For more detailed study, particularly of the approximate magnitude of extension, dikes were measured along selected transects perpendicular to the average dike strike where feasible. Transects ranged from <400 m to >7 km in length. Thinner dikes were measured with a ruler, and thicker (>1 m) dikes were measured with a tape measure or by pacing. The length of a transect was either paced for short transects or calculated from start and end point Universal Transverse Mercator (UTM) data for long transects. Transects perpendicular to the average dike strike were not always practical due to more complete exposure on ridges and road-cuts. In these cases, the bearings were used to correct the length perpendicular to the average strike. The few dikes intruded with a dip of <50° were excluded, as they accommodated little horizontal extension.

Extension (dilation) was calculated using the formula: $E = y/(x–y) * 100$, where E = extension, y = total dike thickness, and x = corrected dike-normal length. It was assumed that opening of dikes was orthogonal to the dike walls and horizontal. We recognize the potential for oblique opening in a transtensional regime, and some of the margins of the Teanaway dikes were sheared, which is compatible with oblique opening. The age and tectonic setting of the shearing is uncertain, however, and dextral separation across dikes of host rock markers, such as beds, compositional layers in metamorphic rocks, or leucocratic sheets in Cretaceous plutons, was not recognized across dikes in any of the domains.

The percentage of extension from diking in the detailed transects was extrapolated to make rough estimates of total extension for different domains. These calculations assumed that the percentages of extension in detailed transects were representative of the dike-normal lengths in the areas near the transects (% extension for transect * dike-normal length = extension).

Errors in the extension calculations arise from multiple sources. Parts of transects are covered and are excluded from the analysis. Dikes are commonly the most resistant rocks, and it is more likely that covered areas largely represent weaker host rock rather than dikes. However, thinner dikes may have been inadequately sampled because they are typically more abundant than thicker ones in some other dike swarms (e.g., Gudmundsson, 1990; Curtis et al., 2008), and this relationship was not reproduced for the Teanaway dikes that were measured. Post-intrusion rotation of strikes and/or dips will also affect the calculated extension direction. Other than for some of the Teanaway dikes, there are insufficient data to restore potential tilt of bedding in host rocks. Paleomagnetic data are only available for the Corbaley Canyon swarm (Stauss, 1982), but results from six Eocene to Miocene plutons in the central and northern Washington Cascades do not indicate regional vertical axis rotation (within uncertainties) relative to North America in the last 47 Ma (Beske et al., 1973; Beck et al., 1982; Fawcett et al., 2003). In addition, some of the shallower dips may result from the inadvertent collection of data from steps in dikes, sills, or faulted surfaces, all of which have been observed. Finally, difficulties in determining thickness in areas of rugged topography also lead to larger human errors, which we assume do not have a systematic bias.

U-Pb Geochronology Methods

A summary of relevant, previously published geochronology from Eocene dikes and associated volcanic rocks and plutons throughout the North Cascades is shown in Table 1 with six new U-Pb zircon chemical abrasion-isotope dilution-thermal ionization mass spectrometry (CA-ID-TIMS) dates for dikes and plutons relevant to this study. The new U-Pb zircon geochronology was produced in the isotope geochemistry laboratory at the Massachusetts Institute of Technology (MIT) and follows the methods described in the appendix to Eddy et al. (2016a) and is only briefly outlined here. All analyses represent individual zircons or individual fragments of zircon. They were spiked with the EARTHTIME [205]Pb-[233]U-[235]U isotopic tracer and analyzed on either the VG Sector 54 or Isotopx Phoenix X62 TIMS at MIT. Mass-dependent instrumental Pb fractionation was corrected using long-term, repeat runs of the NBS-981 Pb isotopic standard for the Isotopx X62 TIMS and using measurements of Pb fractionation on the VG Sector 54 TIMS that leveraged the known [202]Pb/[205]Pb ratio in the EARTHTIME [202]Pb-[205]Pb-[233]U-[235]U isotopic tracer. Mass-dependent instrumental U fractionation was corrected using the known [233]U/[235]U ratio in the EARTHTIME [205]Pb-[233]U-[235]U isotopic tracer and assuming a zircon [238]U/[235]U ratio of 138.818 ± 0.045 (2σ: Hiess et al., 2012). We assume that all Pb_c represents laboratory contamination of each zircon aliquot and correct for this contamination using

Miller et al. | Eocene dike orientations in Washington Cascades

TABLE 1. AGES, ORIENTATIONS, AND EXTENSION DIRECTIONS
OF DIKE SWARMS

Swarm	*Age (Ma)	Average strike	Extension direction
Teanaway	49.341 ± 0.033	036°	126–306°
Corbaley Canyon	46.69 + 0.7/-0.073	119°	029–209°
	[a]47.8 ± 1.9		
	[b]48.4 ± 2.2		
Southern Duncan Hill		058°	148–328°
Eastern Duncan Hill	47.505 ± 0.018	025°	115–295°
		[c]121°	031–211°
Cooper Mountain	49.272 ± 0.040	008°	098–278°
Golden Horn-Monument Peak	48.726 ± 0.027	030°	120–300°
Reconnaissance			
Northern Duncan Hill	46.39 ± 0.06		
Hungry Mountain	[b]44.5 ± 0.9	N-NW	WSW–ENE
Skagit – South		032°	122–302°
Skagit – Central	<48.158 ± 0.023	092°	002–182°
Skagit – North	44.857 ± 0.023	NW	NE–SW

*U-Pb zircon, except for [a] = K-Ar biotite and [b] = K-Ar hornblende.
[c]Smaller maxima.
Note: Sources of ages in text.

the mass of ^{204}Pb and an assumed Pb$_c$ isotopic composition of ^{206}Pb/^{204}Pb = 18.13 ± 0.96 (2σ), ^{207}Pb/^{204}Pb = 15.28 ± 0.60 (2σ), and ^{208}Pb/^{204}Pb = 37.04 ± 1.77 (2σ) based on 149 total procedural blanks run at the MIT isotope geochemistry laboratory. A correction for initial secular disequilibrium in the ^{238}U-^{206}Pb decay chain due to exclusion of Th during zircon crystallization was corrected using the mass of radiogenic ^{208}Pb, assuming concordance between the U-Pb and ^{232}Th-^{208}Pb decay systems to calculate a [Th/U]$_{zircon}$, and using an empirically determined ratio of partition coefficients for Th and U between zircon and silicic melt (f_{ThU} = 0.138: Stelten et al., 2015). All isotopic results are presented in Table 2. Concordia plots are shown in Figure 4.

■ U-Pb GEOCHRONOLOGY RESULTS

We present our preferred date of emplacement for each dike and pluton sample in Tables 1–2. The ^{238}U-^{206}Pb isotopic system provides the most precise dates for rocks of Eocene age, and the Th-corrected ^{206}Pb/^{238}U dates are used for all of our interpretations. We assume that dikes cooled quickly relative to the analytical precision for individual analyses (~20–150 k.y.) and interpret any age heterogeneity to represent the incorporation of antecrysts or xenocrysts

or prolonged magma residence prior to transport by dike. In this case, the youngest zircon is the best estimate for the age of dike emplacement. For dike samples with no resolvable age dispersion, we use a weighted mean and report the resulting mean square of the weighted deviates (MSWD).

Interpreting age heterogeneity in plutonic rocks is more challenging. Age dispersion in these rocks may represent protracted crystallization at the emplacement level (e.g., Samperton et al., 2015), transport of antecrystic zircons from deeper crustal levels (Miller et al., 2007), or incorporation of xenocrysts (Miller et al., 2007). For this study, we interpret grains that are significantly older (>>250 k.y.) than the main age population in a plutonic sample to represent xenocrysts or antecrysts. Grains that cluster to within <200 k.y. are tentatively interpreted to represent crystallization in situ, and consequently we report a mean age and overdispersion (Vermeesch, 2018). In this case, we interpret the overdispersion to approximate the crystallization duration. A single sample (NMNC362) yielded grains that show slight normal discordance (Fig. 4). The cause of this discordance remains unclear, and we refrain from attaching significance to the spread of ages in this sample. Nevertheless, it is the only U-Pb zircon CA-ID-TIMS date for the Railroad Creek pluton, and we interpret that the pluton intruded at ca. 45.5 Ma. Another sample (NC-MPE-414) from the Lost Peak stock has only two zircons dated. Both overlap within uncertainty and provide a date of ca. 49.6 Ma. This data set is too small to adequately assess whether there is age dispersion or inheritance in this sample. However, we tentatively interpret that the Lost Peak stock was emplaced ca. 49.6 Ma and report it here since these are the only modern geochronologic data for this intrusion.

Table 1 also presents previously published geochronologic data from dikes, plutons, and related volcanic rocks that help to constrain the age of dike swarms throughout the region. The data form the basis of our analysis of potential temporal trends in dike orientations and are discussed as needed in the following sections.

■ EOCENE DIKE DOMAINS IN THE WASHINGTON CASCADES

Teanaway Dike Swarm

The Teanaway dikes are the southernmost and most voluminous of the dike swarms and are exposed over ~675 km² (Smith, 1904; Foster, 1958; Tabor et al., 1982, 2000; Doran, 2009). They intrude a ~45-km-long, E-W–trending zone, which has a width averaging ~15 km and ranging from ~8–20 km. The dikes intrude the Paleocene(?)-Eocene Swauk Formation and locally the adjacent Mesozoic Ingalls ophiolite and Mount Stuart batholith (Figs. 3, 5, and 6A). Individual dikes are basalt to diabase, and geochemically they are medium-K tholeiitic basalts and basaltic andesites (Clayton, 1973; Peters and Tepper, 2006; Tepper et al., 2008). Dike thicknesses range from ca. 10 cm to 85 m, but the thickest dikes may be composite and have unrecognized internal contacts; however, no grain-size changes, or multiple columnar rows (cf. Gudmundsson,

Miller et al. | Eocene dike orientations in Washington Cascades

TABLE 2. CHEMICAL ABRASION-ISOTOPE DILUTION-THERMAL IONIZATION MASS SPECTROMETRY U-Pb ZIRCON GEOCHRONOLOGY RESULTS

	Dates (Ma)								Composition				Isotopic ratios						
	$^{206}Pb/^{238}U$ <Th>[a]	±2σ abs	$^{207}Pb/^{235}U$[b]	±2σ abs	$^{207}Pb/^{206}Pb$ <Th>[a]	±2σ abs	Corr. coef.	% disc[c]	Th/U[d]	Pbc (pg)[e]	Pb*/Pbc[f]	Th/U (magma)[g]	$^{206}Pb/^{204}Pb$[h]	$^{208}Pb/^{206}Pb$[i]	$^{206}Pb/^{238}U$[i]	±2σ %	$^{207}Pb/^{235}U$[i]	±2σ %	$^{207}Pb/^{206}Pb$[i]	±2σ %
NC-MPE-414: Lost Peak Stock (48.82093°N 120.49037°W)																			
z1	49.611	0.043	49.45	0.22	41.7	9.5	0.666	-7.02	0.52	0.30	71	3.770	4219	0.167	0.0077110	0.086	0.04991	0.45	0.04696	0.39
z3	49.621	0.052	49.78	0.47	57	22	0.377	19.73	0.38	0.83	24	2.750	1469	0.120	0.0077126	0.11	0.05024	0.97	0.04727	0.94
Emplacement date: 49.6 Ma*																			
NC-MPE-004B: Duncan Hill Pluton (47.98392°N 120.57352°W)																			
z1	46.496	0.025	46.582	0.094	51.0	4.5	0.488	16.91	0.38	0.18	123	2.750	7576	0.123	0.0072241	0.052	0.046945	0.21	0.047152	0.18
z4	46.506	0.030	46.72	0.23	57	12	0.329	25.45	0.30	0.24	43	2.170	2722	0.095	0.0072258	0.064	0.04708	0.50	0.04728	0.49
z2	46.519	0.092	47.3	1.1	87	58	0.331	49.57	0.36	1.80	8	2.610	525	0.115	0.007228	0.20	0.0477	2.5	0.0479	2.4
z5	46.555	0.027	46.67	0.16	52.7	7.9	0.399	19.25	0.32	0.26	63	2.320	3945	0.103	0.0072333	0.056	0.04704	0.35	0.04719	0.33
z3	46.572	0.027	46.72	0.13	54.4	6.5	0.417	21.54	0.26	0.24	82	1.880	5229	0.084	0.0072360	0.056	0.04709	0.29	0.04722	0.27
z6	46.628	0.056	46.98	0.60	65	30	0.332	33.10	0.33	0.46	16	2.390	1022	0.106	0.0072447	0.12	0.04735	1.3	0.04742	1.3
Emplacement date: 46.545 Ma[†]																			
Overdispersion: 0.039 +0.049/–0.021 Ma																			
NMNC362: Railroad Creek Pluton (48.19471°N 120.60720°W)																			
za	45.546	0.026	45.716	0.074	54.7	3.3	0.59	23.73	0.29	0.19	179	2.1	11277	0.092	0.0070757	0.056	0.046053	0.16	0.047226	0.14
zb	45.474	0.038	45.57	0.13	50.4	6.3	0.488	17.99	0.23	0.32	88	1.67	5634	0.075	0.0070645	0.082	0.0459	0.29	0.04714	0.26
zc	45.512	0.024	45.664	0.06	53.7	3.1	0.286	22.45	0.24	0.19	183	1.74	11698	0.078	0.0070704	0.05	0.045999	0.13	0.047205	0.12
zd	45.568	0.038	45.8	0.18	57.9	9.1	0.432	27.58	0.33	0.26	62	2.39	3876	0.106	0.0070792	0.083	0.04614	0.41	0.04729	0.38
Emplacement date: 45.5 Ma[§]																			
NC-MPE-207B: Cooper Mountain–Goat Mountain Porphyry Dikes (48.03329°N 119.98376°W)																			
z1	49.44	0.15	50.1	1.8	80	87	0.352	41.44	0.65	0.68	6	4.71	362	0.207	0.007684	0.31	0.0505	3.8	0.0477	3.7
z2	49.272	0.04	49.26	0.29	49	14	0.364	7.92	0.64	0.6	41	4.64	2345	0.204	0.007658	0.082	0.04971	0.6	0.0471	0.58
z3	49.601	0.044	49.6	0.24	50	11	0.41	8.72	0.36	0.53	47	2.61	2895	0.114	0.0077094	0.088	0.05006	0.49	0.04712	0.46
z4	49.422	0.063	49.71	0.61	64	29	0.403	27.8	0.43	1.03	18	3.12	1096	0.136	0.0076814	0.13	0.05018	1.2	0.0474	1.2
z5	49.411	0.037	49.42	0.1	50.1	4.3	0.579	9.69	0.38	0.63	152	2.75	9368	0.121	0.0076798	0.075	0.04988	0.21	0.047127	0.18
z6	49.278	0.036	49.23	0.15	46.8	6.9	0.452	4.21	0.53	0.3	100	3.84	5908	0.17	0.007659	0.073	0.04968	0.31	0.04706	0.29
z7	49.6	0.052	50.04	0.55	71	26	0.33	34.72	0.39	0.33	19	2.83	1199	0.125	0.0077092	0.11	0.05052	1.1	0.04755	1.1
z8	49.393	0.088	49.4	0.62	50	30	0.341	9.35	0.45	0.22	20	3.26	1211	0.145	0.007677	0.18	0.04986	1.3	0.04712	1.2
Youngest grain: 49.272 ± 0.040/0.046/0.070 Ma																			
NC-MPE-302C: Duncan Hill Dike (47.89358°N 120.21540°W)																			
z1	47.497	0.035	47.61	0.17	53.3	7.9	0.463	18.27	0.55	0.62	68	3.990	3990	0.175	0.0073806	0.074	0.04800	0.36	0.04719	0.33
z2	47.502	0.038	47.62	0.26	54	13	0.403	18.84	0.40	0.59	40	2.900	2483	0.128	0.0073814	0.079	0.04802	0.56	0.04720	0.53
z3	47.511	0.039	47.69	0.31	57	15	0.370	22.90	0.46	1.19	33	3.330	1977	0.148	0.0073827	0.082	0.04809	0.67	0.04726	0.65
z4	47.515	0.048	47.57	0.33	50	16	0.434	13.95	0.49	0.27	36	3.550	2143	0.156	0.0073834	0.10	0.04797	0.72	0.04714	0.68
z5	47.509	0.050	47.56	0.17	50.4	7.7	0.477	13.97	0.59	0.67	73	4.280	4279	0.189	0.0073824	0.11	0.04796	0.36	0.04714	0.32
z6	49.096	0.041	49.21	0.21	54.9	9.6	0.496	17.60	0.39	0.22	65	2.830	3968	0.125	0.0076305	0.083	0.04966	0.43	0.04722	0.40
Weighted mean: 47.505 ± 0.018/0.028/0.058 Ma (n = 5, MSWD = 0.13)[#]																			
NC-MPE-371A: Golden Horn Dike (48.65517°N 120.57148°W)																			
z1	48.694	0.063	48.53	0.66	40	32	0.509	-8.24	0.34	0.16	19	2.460	1176	0.108	0.0075676	0.13	0.04895	1.4	0.04694	1.3
z2	48.681	0.049	48.60	0.43	44	20	0.475	0.88	0.31	0.20	26	2.250	1668	0.100	0.0075656	0.10	0.04902	0.90	0.04702	0.85
z3	48.758	0.083	48.85	0.92	53	45	0.410	15.96	0.30	0.41	11	2.170	721	0.096	0.007578	0.17	0.04928	1.9	0.04719	1.9
z5	48.754	0.043	48.97	0.24	59	11	0.476	24.07	0.30	0.42	44	2.170	2767	0.095	0.0075771	0.087	0.04941	0.51	0.04732	0.47
Weighted mean: 48.726 ± 0.027/0.037/0.064 Ma (n = 4, MSWD = 2.3)																			

[a]Corrected for initial Th/U disequilibrium using radiogenic ^{208}Pb and Th/U[magma] calculated using f_{ThU} = 0.138 (Stelten et al., 2015).
[b]Isotopic dates calculated using λ238 = 1.55125E-10 (Jaffey et al., 1971) and λ235 = 9.8485E-10 (Jaffey et al., 1971).
[c]% discordance = 100 – (100 * ($^{206}Pb/^{238}U$ date) / ($^{207}Pb/^{206}Pb$ date)).
[d]Th contents calculated from radiogenic ^{208}Pb and ^{230}Th-corrected $^{206}Pb/^{238}U$ date of the sample, assuming concordance between U-Pb Th-Pb systems.
[e]Total mass of common Pb.
[f]Ratio of radiogenic Pb (including ^{208}Pb) to common Pb.
[g]Th/U ratio of magma from which mineral crystallized.
[h]Measured ratio corrected for fractionation and spike contribution only.
[i]Measured ratios corrected for fractionation, tracer, and blank.
*Only two zircons were dated from this sample. However, since it is the only modern geochronologic measurement for this unit, we include the data here but do not assign a more precise date than 49.6 Ma.
[†]Calculated using the algorithms for overdispersed data in Vermeesch (2018).
[§]Slight normal discordance could be due to initial Pa excess or subtle inheritance. Due to this uncertainty, we do not assign an emplacement date more precise than 45.5 Ma.
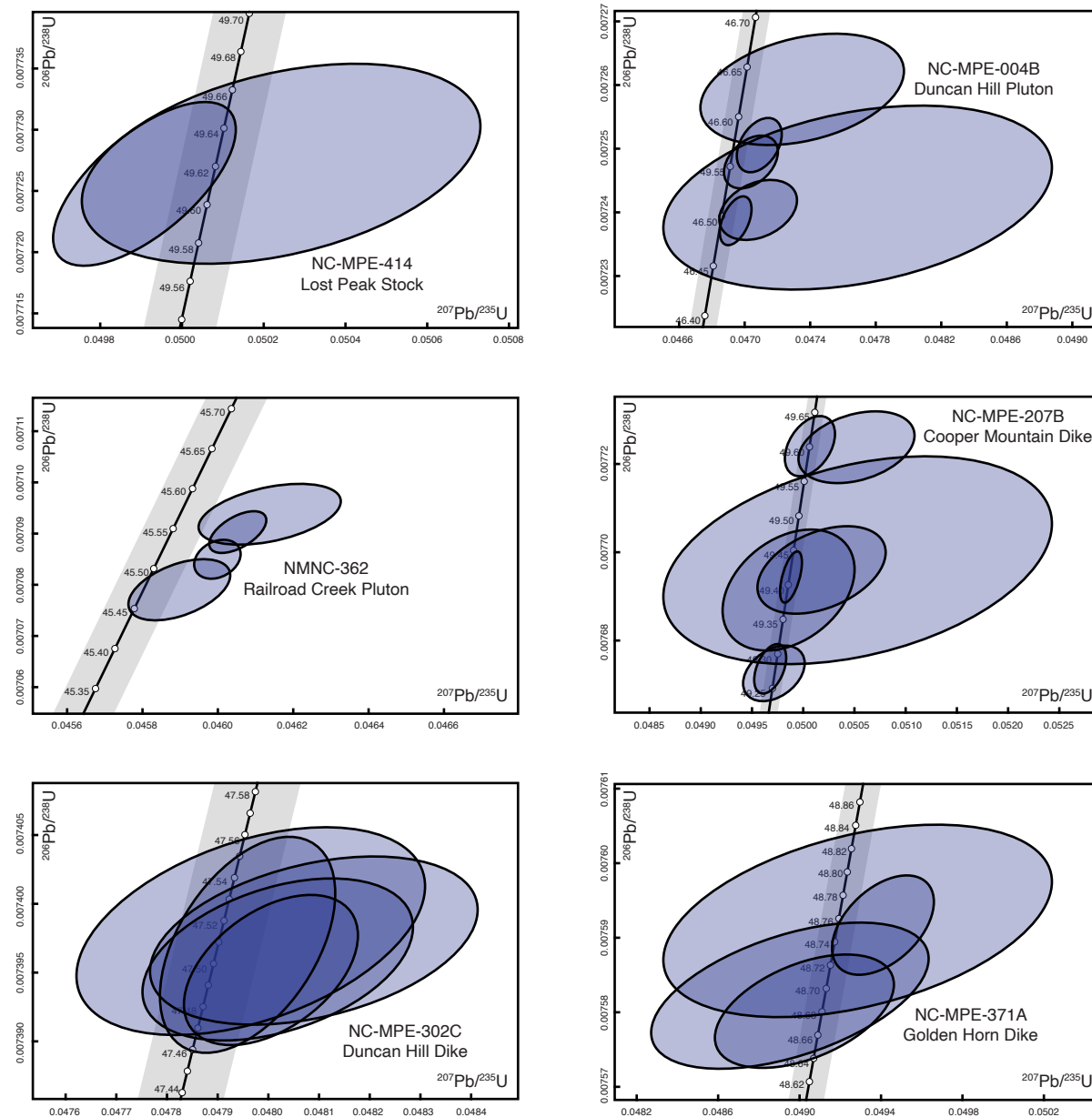[#]One anomalously old zircon (z6) was excluded from the weighted mean calculation.

Figure 4. U-Pb zircon concordia plots for Eocene dikes and plutons are shown. (A) Lost Peak stock (49.6 Ma). (B) Duncan Hill pluton (46.5 Ma). (C) Railroad Creek pluton (45.5 Ma). (D) Cooper Mountain dike (49.272 Ma). (E) Duncan Hill dike (47.505 Ma). (F) Golden Horn–Monument Peak dike (48.726 Ma).
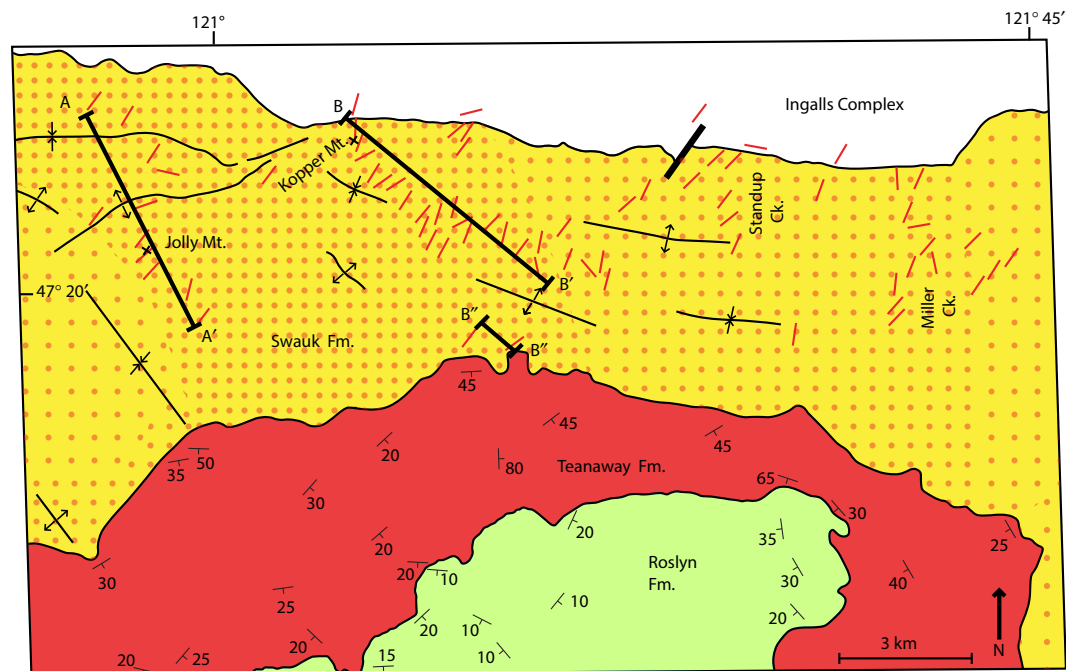
Miller et al. | Eocene dike orientations in Washington Cascades

Figure 5. Simplified map emphasizes strikes and concentrations of Teanaway dikes in the central part of the Teanaway swarm. Spacing of dots reflects dike concentration, which reaches 60–80% in some areas. The locations of transects discussed in the text are shown except for the Cle Elum River transect, which is a few kilometers west of the map. A–A' and B–B' show the detailed transects for which extension was calculated. Dike strikes are from our data, and concentrations are from Tabor et al. (1982, 2000) and us. Note the attitudes of beds in the unconformably overlying Teanaway Formation, which facilitate rotation of dikes to their original orientations. Fold axes are from Tabor et al. (1982, 2000), Doran (2009), and Gundersen (2017). Ck.—creek.

1995), have been recognized. Many Teanaway dikes are segmented, as is typical of dikes (e.g., Delaney and Pollard, 1981), and the longest dikes extend along strike for ≥3 km (Foster, 1958).

The dikes are likely related to the nearby Teanaway Formation, which unconformably overlies the Swauk Formation and consists predominantly of subaerial basalts and minor rhyolites (Smith, 1904; Foster, 1958; Clayton, 1973; Tabor et al., 1982). Clayton (1973) suggested that the dikes were a feeder system to a large shield volcano in the southwestern part of the Teanaway Formation. Dikes do not cut the overlying middle to late Eocene (maximum depositional age of 48.80 ± 0.11 Ma; Eddy et al., 2016a) Roslyn Formation, or the Chumstick basin, which contains a 49.1 Ma tuff and lays on the east side of the Leavenworth fault (Fig. 3). These observations imply that the dikes were emplaced after deposition of the ≤59 Ma–ca. 51 Ma Swauk Formation and during eruption of the Teanaway Formation. A rhyolite near the base of the Teanaway Formation is 49.341 ± 0.033 Ma (U-Pb zircon) and provides the best estimate for the age of the dikes (Eddy et al., 2016a).

A total of 319 dike orientations were measured in the Teanaway swarm, the majority of which were taken in five NW-SE– to N-S–trending transects across the swarm (Fig. 5), and the largest number of measurements was in the narrow, central portion of the Swauk Formation, where dikes are most abundant (Tabor et al., 1982). Thicknesses were measured for most of these

dikes, particularly in two transects (Jolly Mountain and Koppen Mountain) for which extension was calculated. Our data are supplemented by 145 dike orientations in the easternmost part of the swarm summarized by Mendoza (2008). Dikes mostly strike NNE to NE (Figs. 5 and 7A; Table 3). Dips range from 90° to 21°, the mean dip is 67°, and dips are generally NW to W–NW. There is no apparent systematic change in dip direction or magnitude between or along our detailed transects. Discounting dikes that dip <40°, the mean strike on a rose diagram is 036° (Fig. 7A) (n = 313), which is close to the mean orientation of 040° for dikes in the eastern part of the swarm (Mendoza, 2008).

Teanaway dikes were tilted after emplacement. The mean dike dip of 67° NW differs from the expected sub-vertical orientation during intrusion, and sparse bedding within the Teanaway Formation typically dips 25° to 30° to the south near the central part of the Swauk Formation. The dikes cut open to tight, upright folds in the Swauk Formation (Table 4), which is consistent with the angular unconformity between the Swauk and Teanaway rocks. Tilt of the Teanaway Formation and dikes results from a younger regional (>25 km wavelength), shallow SE-plunging, gentle syncline (Tabor et al., 1982, 2000). The initial orientation of dikes was approximated by taking the average attitude of bedding in the Teanaway Formation and rotating the bedding and unconformity back to horizontal. Regional variation in bedding strike was accounted for by using the average local strike and dip south of dike transects. After
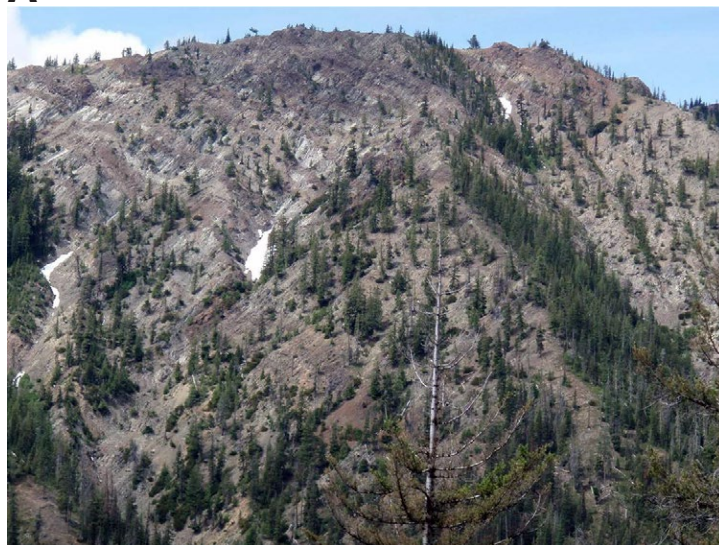
Figure 6. Field photographs show dike swarms. (A) Teanaway dikes (brown) in Miller Creek domain. Lighter-colored areas are screens of sandstone of the Swauk Formation. Dikes make up >50% of the outcrop. Trees (most are >20 m tall) provide scale. (B) Corbaley Canyon dikes form resistant fins as viewed from the other (west) side of the Columbia River. (C) Resistant dikes in the eastern Duncan Hill domain on Google Earth image. Dikes trend NE (note N arrow), and some extend at least 2 km. (D) Golden Horn dike (orange weathering) intrudes the Cretaceous Black Peak batholith. Relief is ca. 700 m.

Miller et al. | Eocene dike orientations in Washington Cascades
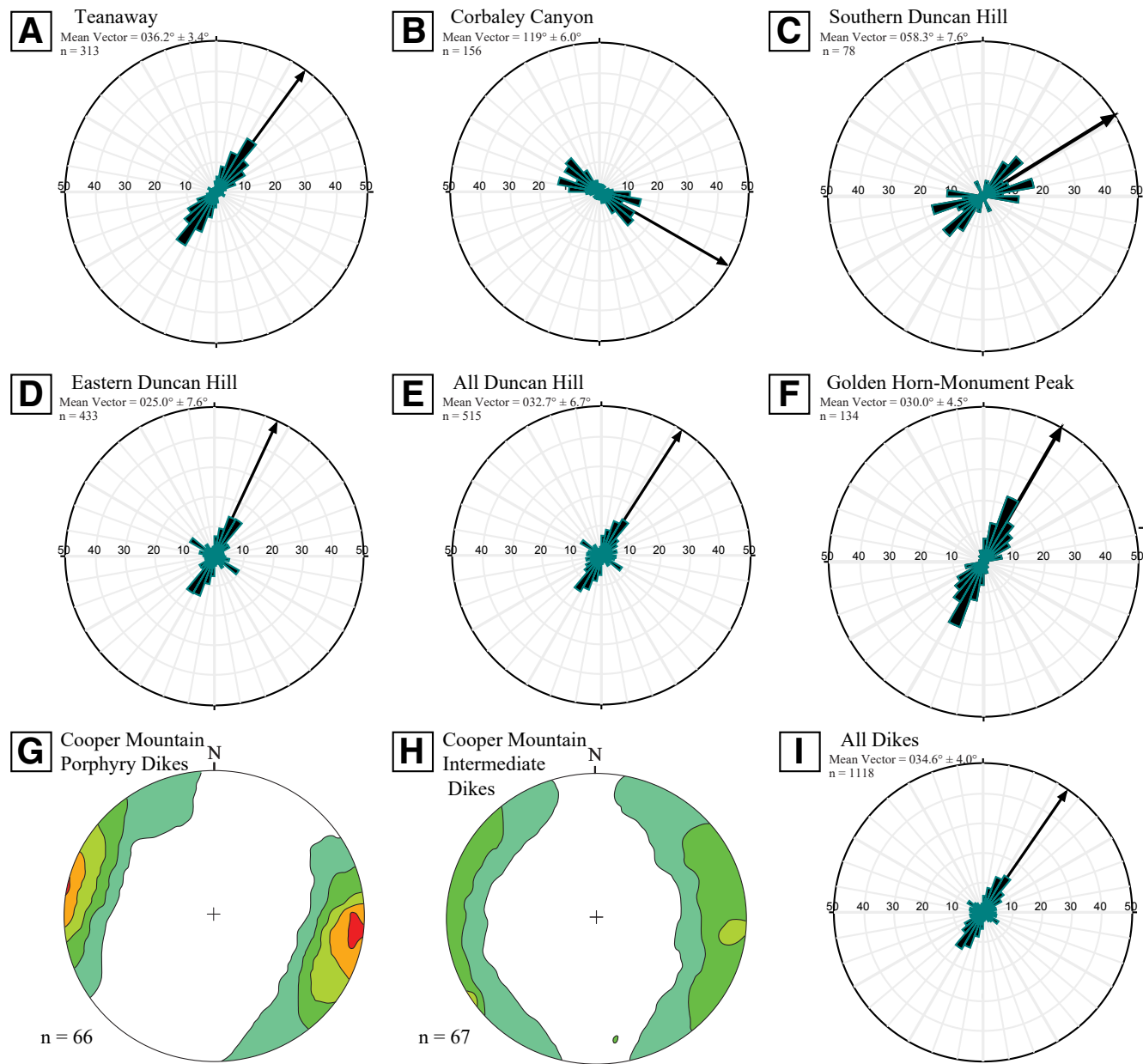
Figure 7. Rose diagrams show strikes of dikes in different domains. Gently dipping dikes are excluded. Note that the Cooper Mountain dikes are shown on lower hemisphere stereographic projections (Raviola, 1988), as the original data are not available.

TABLE 3. TRANSECTS ACROSS THE TEANAWAY DIKE SWARM

Transect	Number of dikes	Mean thickness (m)	Mean orientation
Cle Elum River	45		*038/85
West–Jolly Mountain	48	19	*031/87
W-Central–Koppen Mountain	103	17	*206/85
E-Central–Standup Creek	46		219/78
E-Central–Miller Creek	57		203/73
East (Highway 97 Area)**		14	040/?

*Rotated, using unconformity.
**Mendoza (2008).

restoration (Table 3), dips for the three western transects range from 85° to 87°, which better fits the expected subvertical dike dips. Dips in the Standup and Miller Creek transects are much more difficult to restore. The few beds measured have significantly different attitudes south of the Standup Creek transect, and the Miller Creek transect extends northward from the sharp bend in the Teanaway–Swauk contact, and beds in the Teanaway Formation and presumably the unconformity are not consistent (Fig. 5). Overall, mean strikes of the five transects fall within a 16° range (Table 3). Rotations of dikes measured by Mendoza (2008) in the large eastern part of the Teanaway swarm are not known, as the orientations of the few measured beds in the Teanaway Formation south of her study area vary considerably, and we do not know the locations of the dikes measured.

Mean dike thicknesses for individual transects range from 12 m to 20 m. Analysis of mean dike thickness at 500 m increments along the well-exposed Jolly Mountain and Koppen Mountain transects indicates that there is no systematic change in thickness across strike, but on average, dikes are thicker in the southeastern half of each transect (Fig. 8) as the Swauk–Teanaway contact is approached.

The magnitudes of extension from dike emplacement were calculated for the Jolly Mountain and Koppen Mountain transects. Dikes (n = 48) in the ~5.35-km-long Jolly Mountain transect accommodated ~17% extension, and dikes (n = 103) in the ~7.13-km-long Koppen Mountain transect recorded ~45% extension (Table 5). Extension magnitudes for the eastern part of the swarm near Highway 97 are ~10.5% (Mendoza, 2008).

Corbaley Canyon Domain Dikes

The dikes of this area and those described below were studied to test the relation between dike orientations and relatively nearby plutons. In Corbaley Canyon and on the west side of the Columbia River (Figs. 3 and 9), lamprophyre to rhyolite dikes with a wide range of textures are common (Waters, 1927; Tabor et al., 1987). More mafic dikes are cut by more felsic dikes in places (Waters, 1927). The different dike compositions in the swarm are interpreted to

TABLE 4. DIKE HOST ROCK UNITS, ROCK TYPES, AND STRUCTURES

Dikes	Main host rock unit(s)	Rock types	Structural orientations
Teanaway	Swauk Formation	Sandstone, mudstone	E-W– to NW-SE–trending folds of bedding
Corbaley Canyon	Swakane Gneiss	Biotite gneiss	Foliation strikes W-NW; dips 40–60° NNE
	Napeequa complex	Quartzite, amphibolite, biotite schist	
	Entiat pluton	Tonalite	
Southern Duncan Hill	Chelan Complex	Tonalitic gneiss	Foliation strikes E-W, NE, and NW; gentle to moderate dips
Eastern Duncan Hill	Chelan Complex	Tonalitic gneiss	Foliations generally strike E-W, some strike N-NW; dips mostly 40–70°S
	Twentyfive Mile Creek Schist	Biotite-hornblende schist	
Cooper Mountain	Twentyfive Mile Creek Schist	Biotite-hornblende schist	Foliation strikes E-W to ENE and locally N-NW; dips generally 30–50° to S and SE
	Orthogneiss	Tonalitic orthogneiss	
	Alta Lake Complex	Amphibolite, biotite schist, leucotonalite	
Golden Horn-Monument Peak	Methow Sequence	Sandstone, mudstone	Beds and foliation mostly strike NW and dip NE;
	Black Pk. Pluton	Tonalite	N-NW– to NW–trending thrusts and folds; E-W faults with sinistral separation
Northern Duncan Hill	Cardinal Pk. and Seven-Fingered Jack plutons	Tonalite	Foliation mostly strikes NW
Southern Skagit Gneiss	Skagit orthogneiss	Tonalitic orthogneiss	Foliation strikes NW; dips SW and NE
Central Skagit Gneiss	Skagit orthogneiss	Tonalitic orthogneiss	Foliation strikes N; dips mostly E
Skagit granitic dikes	Skagit orthogneiss	Tonalitic orthogneiss	Foliation strikes NW; moderate SW and NE dips

Jolly Mountain Transect
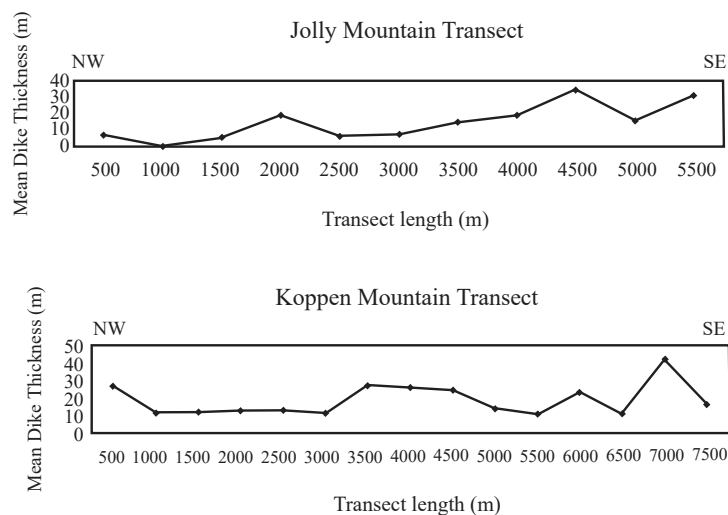

Koppen Mountain Transect

Figure 8. Mean dike thicknesses along the Jolly Mountain and Koppen Mountain transects in the Teanaway domain are shown. Thicknesses are plotted every 500 m along the transects. The locations of transects are shown in Figure 5.
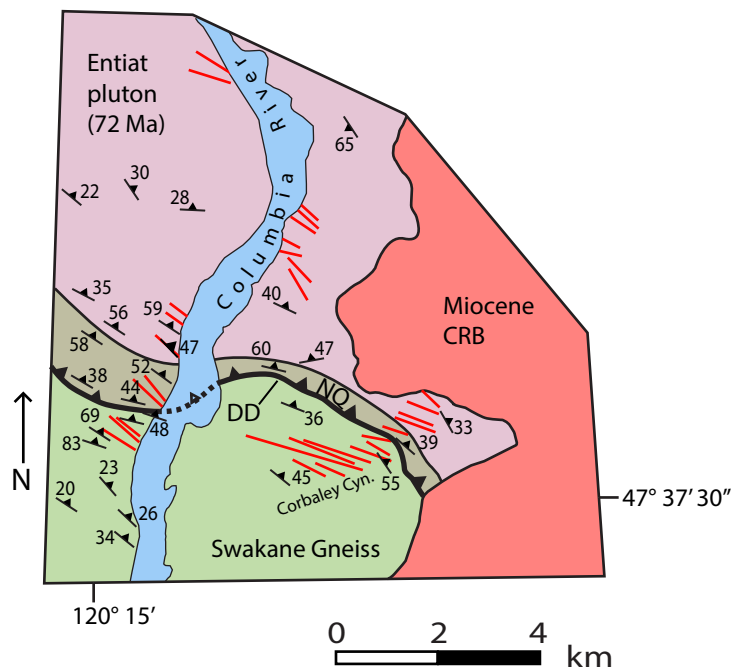

Figure 9. Map shows dike and foliation orientations in the Corbaley Canyon domain. CRB—Columbia River Basalt Group; DD—Dinkelman décollement; NQ—Napeequa unit. Map is modified from Tabor et al. (1987).

TABLE 5. MAGNITUDES OF EXTENSION

Swarm	Length (m)	# dikes	Total dike thickness (m)	% extension
Teanaway–Jolly Mountain	5350	41	770	16.8
Teanaway–Koppen Mountain	7130	127	2210	44.9
Corbaley Canyon–In Canyon	1218	N.A.	312	34.3
Corbaley Canyon– W of Columbia River	2446	N.A.	147	6.4
S. Duncan Hill	381	N.A.	47	14.1
E. Duncan Hill	480	30	22	4.8
Cooper Mountain	2034	180	900	79.4
N.A.—not available.				

record differentiation from a single magmatic source (Waters, 1927; Loewen et al., 2006). Dikes mainly intrude the metapsammitic Swakane Biotite Gneiss, quartzite, amphibolite, and biotite schist of the Napeequa unit, and the 72 Ma tonalitic Entiat pluton (Fig. 9). Two K-Ar dates of 48.4 ± 2.2 Ma and 47.8 ± 1.9 Ma for hornblende and biotite, respectively (Tabor et al., 1987), and a U-Pb LA-ICP-MS age for zircon of 46.69 +0.70/–0.73 Ma (J. Tepper, 2018, personal commun.) date the dikes.

Dikes in Corbaley Canyon average ca. 7–10 m in thickness, and Waters (1927) describes an ~30-m-wide composite dike consisting of four chemically distinct rock types. Individual dikes can be traced for as much as 3 km (Fig. 6B). Dikes thin to the west of the Columbia River, where they are typically <50 cm thick, although a few large ones reach 15 m in width.

Strikes (n = 156) of dikes in the Corbaley Canyon domain have a mean rose vector of 119°; dips average 74° and are mostly S-SW (Fig. 7B). The dikes were at least slightly tilted, as dips of unconformably overlying basalt flows of the Miocene Columbia River Group near Corbaley Canyon average ~8°, but dip direction is very inconsistent (Tabor et al., 1987), which makes restoration of the unconformity and dikes problematic. The regional antiform that folds the Swakane and Napeequa rocks and intervening Dinkelman décollement may have caused much more tilting, but the relative timing of this folding and diking is uncertain. The folding is post-72 Ma and probably post-ca. 50 Ma, but its younger limit is only constrained as predating the 16 Ma Columbia River basalts (Paterson et al., 2004). If the folding is synchronous with that of the Swauk Formation during collision of Siletzia, then it would predate the dikes. Alternatively, if folding is younger then the dikes, then the S-SW–dipping dikes

would rotate to steeper dips if the moderately N-NE–dipping foliation in host rocks was rotated back to a gentler, but uncertain, pre-folding dip. Paleomagnetic data from the dikes are also difficult to interpret. Stauss (1982) found discordance from the Eocene paleopole, but without information on paleohorizontal during intrusion or other geologic evidence, a conclusion about the mechanism responsible for the discordance was not reached. If the discordance was caused entirely by vertical axis rotation, then ~142° of clockwise rotation is needed (Harrison, 1984). These uncertainties clearly complicate the interpretations of original strikes and dips of dikes.

Nine transects surveyed within Corbaley Canyon have a total corrected length of ~1.2 km. The cumulative horizontal extension from these transects is ~34% (Table 5). In contrast, 11 transects on the west side of the Columbia River have a total corrected length of ~2.4 km, extension for individual transects ranges from <1% to 20%, and the cumulative extension is only ~6% (Table 5).

Southern Duncan Hill Dikes

Tabor et al. (1987) mapped a >200 km^2 area of abundant rhyolite, granite porphyry, and intermediate to mafic dikes intruding the Cascades core west of the Columbia River and concentrated near the shallow (~2.2–3.5 km paleodepth) SE end of the tilted Eocene (46.5 ± 0.2 Ma; U-Pb zircon) (Fig. 3) Duncan Hill pluton (Fig. 10) (Dellinger, 1996). These dikes have not been dated, but a granite porphyry dike intruding rocks SW of the Duncan Hill pluton and ~6 km NW of the southern Duncan Hill domain yields a K-Ar biotite date of 47.0 ± 0.7 Ma (Tabor et al., 1987). Dikes in the southern Duncan Hill domain are hosted by poorly exposed tonalitic gneiss of the Cretaceous Chelan Complex (Fig. 10; Tabor et al., 1987).

Dikes (n = 74) in this domain have a mean strike of 058° (Fig. 7D), and there is a somewhat bimodal distribution of strikes at ca. 210–220° and 240–250°.
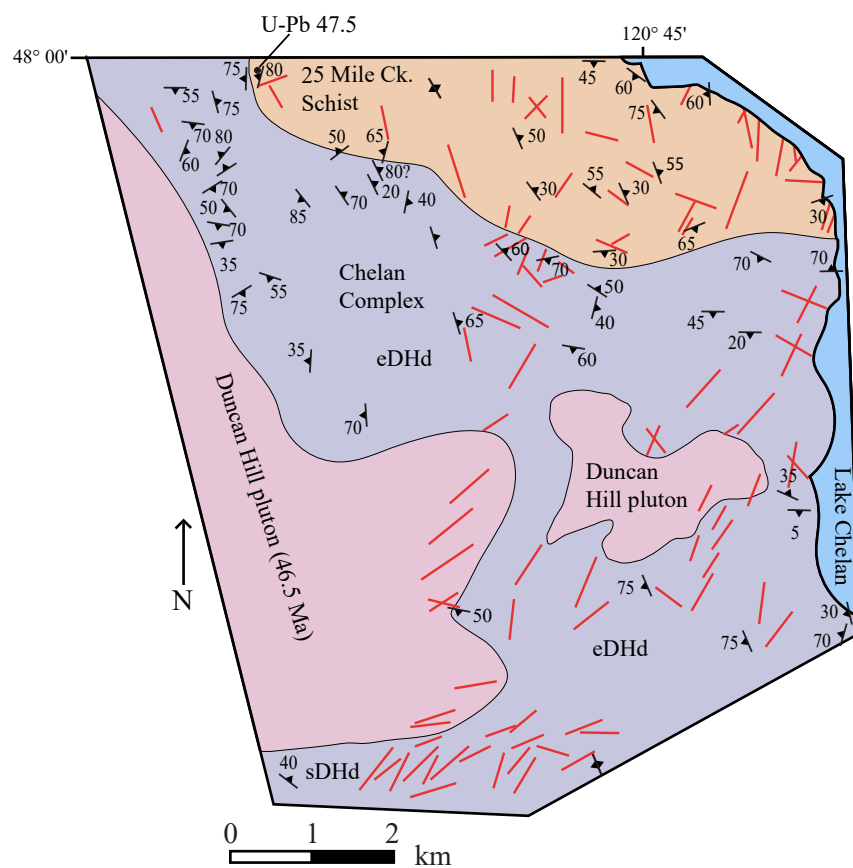

Figure 10. Map shows dike and foliation orientations in the southern (sDHd) and eastern (eDHd) Duncan Hill domains. Location of dated dike in the eastern domain is also shown (dot labeled "U-Pb 47.5"). Map modified from Tabor et al. (1987). Ck.—creek.

Some of the dikes within 1 km of the pluton are roughly subparallel to the E-NE–trending margin (Fig. 10). Dips are mostly NW and >60°.

Ten short transects analyzed near the southern margin of the Duncan Hill pluton provide a total length of ~381 m. The cumulative extension is ~14% (Table 5).

Eastern Duncan Hill Dikes

We conducted a detailed study of dikes in an ~80 km² area on the east side of the Duncan Hill pluton (Fig. 10) (see Bryant, 2017, for details). Intermediate to mafic dikes dominate over granitic porphyry and rhyolite dikes. Dikes average ~1 m in thickness. A granitic porphyry dike from this domain is 47.505 ± 0.018 Ma (U-Pb zircon) (Fig. 4). Dikes in the eastern Duncan Hill domain intrude the Chelan Complex and biotite-hornblende schist and gneiss of the Twentyfive Mile Creek Schist (Tabor et al., 1987; Hopson and Mattinson, 1994).

Orientations of 438 dikes were measured. Data analysis included evaluation of the spatial distribution of dike strikes relative to the margin of the Duncan Hill pluton to test the hypothesis that there is a genetic relationship between the dikes, their orientation, and the pluton (Hopson et al., 1987; Dellinger, 1996). Strikes of 74 of the dikes were approximated using Google Earth (Fig. 6C). Dike strikes vary considerably. The mean vector strike for all dikes measured (excluding a few with shallow dips) is 025° (Fig. 7D) and dips average ~75° SE. A much smaller maxima strikes WNW (301°) and dips steeply NNE. Dike orientations were subdivided on the basis of distance from the Duncan Hill pluton by Bryant (2017). Dikes (n = 111) within 3 km of the pluton have a mean strike of 027°, whereas those farther from the pluton have a mean of 021°. The smaller WNW maxima varies less with distance.

The potential influence of host rock lithology, combined with distance from the Duncan Hill pluton, was also considered (Bryant, 2017). The average strikes of dikes intruding the strongly foliated Twentyfive Mile Creek schist are NW (~310°; n = 57 dikes) within 5 km of the Duncan Hill pluton and swing to E-W (087°; n = 66 dikes) at distances of 5–10 km from the pluton (Bryant, 2017). In contrast, dikes intruding the weakly to moderately foliated Chelan Complex consistently strike NE (~038°; n = 136) within 10 km of the pluton (Fig. 10) (Bryant, 2017).

The magnitude of magmatic extension was calculated from two well-exposed transects east of the Duncan Hill pluton. The combined length was ~480 m, and there was ~5% extension (Table 5).

Cooper Mountain Dikes

Numerous dikes intrude near the granodioritic, ca. 49–48 Ma Cooper Mountain batholith and the area between this intrusion and the Duncan Hill pluton (Raviola, 1988) (Fig. 11). These dikes include porphyritic granodiorite and granite dikes and a swarm of mafic dikes that range from basalt to hornblende lamprophyre (spessartite). The porphyritic dikes are similar in mineralogy to the Cooper Mountain rocks, and the mafic dikes are similar petrographically to those E and SE of the Duncan Hill pluton (Raviola, 1988; Hopson and Mattinson, 1994). A U-Pb zircon age (49.272 ± 0.040 Ma; Table 2) of a dike intruding the southern margin of the Cooper Mountain batholith is older than the U-Pb age of 47.88 ± 0.36 Ma from the northwestern margin (Shea, 2008). A dike intruding host rocks south of the pluton gave a K-Ar hornblende date of 48.1 ± 1.3 Ma (Tabor et al., 1987). The mafic dikes cut the porphyritic dikes, and the porphyries appear to locally back-vein into the mafic dikes, which suggests that they are in part co-magmatic.

Individual porphyritic dikes vary from ~50 cm to >30 m in thickness and average 8–10 m, whereas mafic dikes range from 10 cm to ≥2 m in thickness and average 1 m. Some of the porphyritic dikes extend for several hundreds of meters along strike. Porphyritic dike thickness and abundance decrease away from the batholith.

The host rocks to the dikes S and SE of the Cooper Mountain batholith include the Twentyfive Mile Creek Schist and orthogneiss of the Cascades core on the SW, and the Alta Lake Complex, which consists of amphibolite, biotite schist, and trondhjemitic sheets, on the SE (Barksdale, 1975; Tabor et al., 1987; Raviola, 1988).

The porphyritic dikes (n = 66) generally strike NNE (010–015°), and dips are commonly ≥75° (Fig. 7G). The mafic dikes (n = 67) vary more in strike; the majority strike ~N-S, but some strike NW (~315°) (Fig. 7H). Many mafic dikes have slightly shallower dips than the porphyritic dikes. The porphyritic dikes are oriented subparallel to the southeast margin of the Cooper Mountain batholith (Fig. 11). Paleomagnetic data from the batholith indicate that it has not been significantly reoriented (Fawcett et al., 2003).

The magnitude of extension near the southern margin of the Cooper Mountain batholith is large. The greatest concentration of dikes is near Goat Mountain (Fig. 11), where dikes locally form 100% of the outcrop over a distance of ~200 m across strike. In this area, ~80 porphyritic dikes and 100 mafic dikes intruded over an across-strike distance of ~2030 m. A rough estimate of the combined extension from the dikes is ~79% (Table 5). This value is almost certainly much higher than for the dike swarm as a whole, as our mapping indicates that the density of dikes decreases to the W and S.

Dikes are also abundant near the SW margin of the Cooper Mountain batholith. Reconnaissance measurements indicate that in at least a few localities of concentrated dikes, strikes are ca. 300°, which is similar to the secondary maxima in the Duncan Hill domain <5 km to the SW. A granite porphyry dike in this area yields K-Ar dates of 44.2 ± 2.0 Ma (hornblende) and 46.9 ± 0.6 Ma (biotite) (Tabor et al., 1987).

The northeastern margin of the Cooper Mountain batholith and Mesozoic rocks of the Methow basin near the Foggy Dew fault of the Ross Lake fault zone (Fig. 3) are intruded by quartz diorite porphyry dikes that are interpreted to be co-magmatic with the 44.5 ± 0.9 Ma (K-Ar hornblende; J. Saburamaru and R. Fleck, unpublished data cited in Hopkins [1987]) Hungry Mountain stock (Hopkins, 1987). Hopkins (1987) named these the South Fork Gold Creek porphyry dikes, recognized ~25 of them, and traced some for several kilometers along strike. These dikes are 2–10 m in thickness and strike N–NW (Hopkins, 1987).
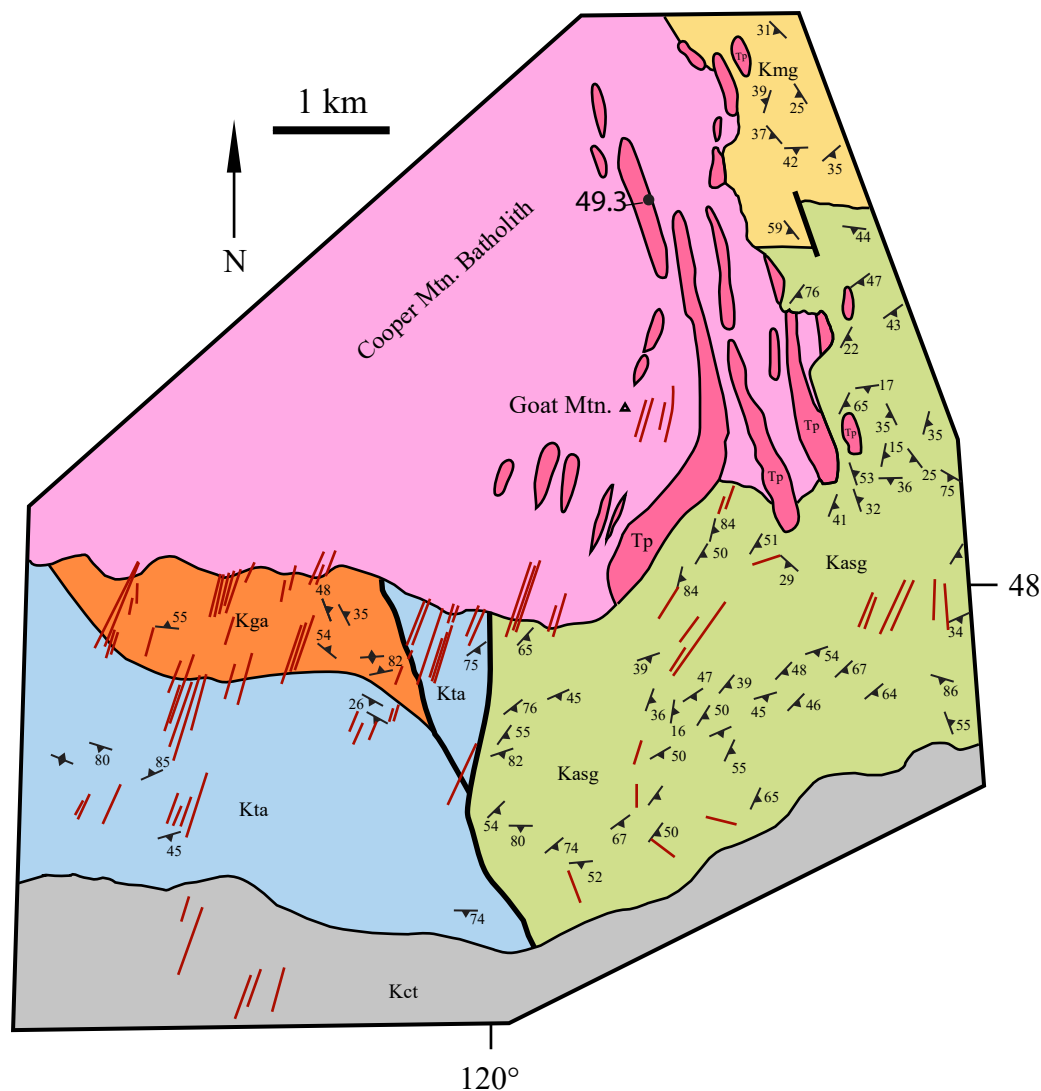
Figure 11. Map shows dike and foliation orientations and the location of the dated dike in the Cooper Mountain domain. Kasg—amphibolite, schist, and gneiss of Alta Lake; Kct—Chelan Complex tonalite; Kga—Antoine Creek gneiss; Kta—amphibolite and schist of Twentyfive Mile Creek; Kmg—Cretaceous Methow Gneiss; Tp—Eocene porphyritic dikes. Map is modified from Raviola (1988) and Stoffel et al. (1991).

Golden Horn-Monument Peak Dikes

Dikes are abundant near the 48.468 ± 0.030–47.729 ± 0.015 Ma (U-Pb zircon; Eddy et al., 2016b) Golden Horn batholith and 47.9 ± 1.4 Ma (K-Ar biotite) Monument Peak stock (Tabor et al., 1968), which are ~15 km apart in map view. Dikes near the Golden Horn batholith include granitic porphyries and fine-grained, intermediate to mafic dikes; most dikes related to the Monument Peak stock are granitic porphyries and quartz porphyries (rhyolites to rhyodacites; Tabor et al., 1968). One dike between the Golden Horn batholith and Monument Peak stock is 48.726 ± 0.027 Ma (U-Pb zircon) (Figs. 4 and 12), which is apparently older than both of these intrusions. Host rocks to the dikes include the Cascades core on the west and Methow

strata on the east (Fig. 12), where dikes also intrude the ca. 49.6 Ma Lost Peak stock (Fig. 4).

The dikes range from <1 m to ~80 m in thickness, and a few can be traced for >3 km along strike (Tabor et al., 1968). Tabor et al. (1968, their fig. 4) show on a sketch map ~134 dikes between the plutons and next to the northern and eastern margins of the Monument Peak stock (Fig. 12). They dominantly trend NE (~030°; Fig. 7F) and include some roughly N-S–trending and a few NW-trending dikes. A 65-m-wide section consisting entirely of dikes intruding Methow strata illustrates the complexity of diking between the Golden Horn and Monument Peak intrusions. The oldest dikes in this section are plagioclase porphyries, which form screens between intermediate and mafic dikes and microgranite dikes. Strikes for 12 of the dikes range from 351° to 057°, and average 024°.

Dikes intrude the Cretaceous Black Peak batholith and metamorphic rocks on the S and SW sides of the Golden Horn batholith (Fig. 12) in an area where the contact of the Golden Horn batholith is offset by ~E-W–striking faults with sinistral separation. Some of these dikes are intermediate to mafic in composition. These dikes strike E-W to W-NW to locally NW (P. Misch, unpublished map in Misch archives, University of Washington Library; Scudder, 2018; our data) in contrast to the dominantly NE strikes on the NE side of the batholith. Paleomagnetic data suggest ~23° of down-to-the-N tilting of the Golden Horn batholith, which has been attributed to deformation in the Ross Lake fault zone (Petro et al., 2002).

Eocene Dikes Elsewhere in the North Cascades

Dikes of various compositions intrude other parts of the Chelan block. Many of the dikes dated are Eocene, but Miocene dikes are also present (Tabor et al., 1987, 2003). We collected reconnaissance data on dike orientations within 10 km of the northern part of the Duncan Hill pluton. These presumed Eocene dikes intrude the Cretaceous Seven Fingered Jack and Cardinal Peak plutons (Fig. 3). Most of the dikes measured strike NE, and undated "Tertiary dikes" shown on 15 minute quadrangle maps N and NE of the Duncan Hill pluton (Cater and Crowder, 1967; Cater and Wright, 1967) have an average trend of 033°. Dikes are locally ductilely deformed, including a 46.39 ± 0.06 Ma (U-Pb zircon) dike (Matzel, 2004) with covered contacts. It has a NW-striking foliation.

Poorly dated dikes intrude 76–48 Ma orthogneisses in parts of the southern and central Skagit Gneiss Complex (Fig. 3) (Michels, 2008; Shea, 2008). The southern dikes (n = 49) have a mean trend of 032° (Shea, 2008). Approximately 25 km to the NW, andesitic to rhyodacitic dikes (n = 33) intrude orthogneisses as young as 48.158 ± 0.032 Ma (U-Pb zircon) and have a mean trend of 092° (Michels, 2008; Miller et al., 2016).

Granitic dikes dated at 44.857 ± 0.023 Ma (U-Pb zircon; Miller et al., 2016) and ca. 45 Ma (U-Pb zircon; Haugerud et al., 1991a) intrude the northern part of the Skagit Gneiss Complex. These dikes have strong, gently NW- and SE-plunging, solid-state lineation but are weakly foliated and cut the typically moderately dipping foliation in the host gneisses (e.g., Misch, 1967; Haugerud et al., 1991a; Wintzer, 2012). They strike NW and dip steeply, but more specific orientations have not been reported.

■ DISCUSSION

Magnitudes of Extension

Magnitudes of horizontal extension (dilation) were calculated in well-exposed transects of the major swarms except for the Golden Horn-Monument Peak dikes (Table 5). The largest calculated extensions are from one of the Teanaway transects and the Cooper Mountain transect, which are compatible with qualitative observations. Approximate extensions in two detailed transects in the Teanaway swarm are 17% and 45%, respectively (Table 5) (Doran, 2009). If the values for these detailed transects are representative of the dike-normal length of the area near the transects, then the average value of 31% extension, combined with the lower ca. 10% extension in the east calculated by Mendoza (2008), gives W-NW–E-SE magmatic extension of ca. 8–9 km. Dikes also occur west of our transects, but the abundance of dikes decreases (Tabor et al., 2000).

The average extension of ~34% for the dikes in Corbaley Canyon is comparable to that of the Teanaway dikes, but these dikes intrude a much smaller area and probably accommodated <1 km of extension. Dikes on the west side of the Columbia River in the Corbaley Canyon domain account for only ~6% extension, which results in ~500 m of NE-SW extension.

Dikes in the southern Duncan Hill domain transects record ~14% extension, whereas on the basis of two transects of limited length, the NE-striking dikes in the eastern Duncan Hill domain account for ca. 5% extension. If these values are representative of the Duncan Hill domains, than diking accommodated ca. 1.0–1.5 km of NW-SE extension.

Magmatic extension by intrusion of the Cooper Mountain dikes is significant in at least some domains, which include in the transect where it is estimated to reach ~79%. This value corresponds to ~900 m of extension. Dikes are common west of this transect, and more work is needed to quantify extension there.

Collectively, the minimum magmatic extension by diking is probably ~12 km. The Golden Horn-Monument Peak dikes, western part of the Cooper Mountain domain, and other less studied dikes not included in this analysis would presumably add at least several kilometers to this estimate.

Relationships between Dikes and Plutons

Previous workers have suggested that several Eocene plutons and dike swarms are genetically related (e.g., Hopson et al., 1987; Misch, 1966) on the basis of proximity. However, most of these dike swarms range from basalt to
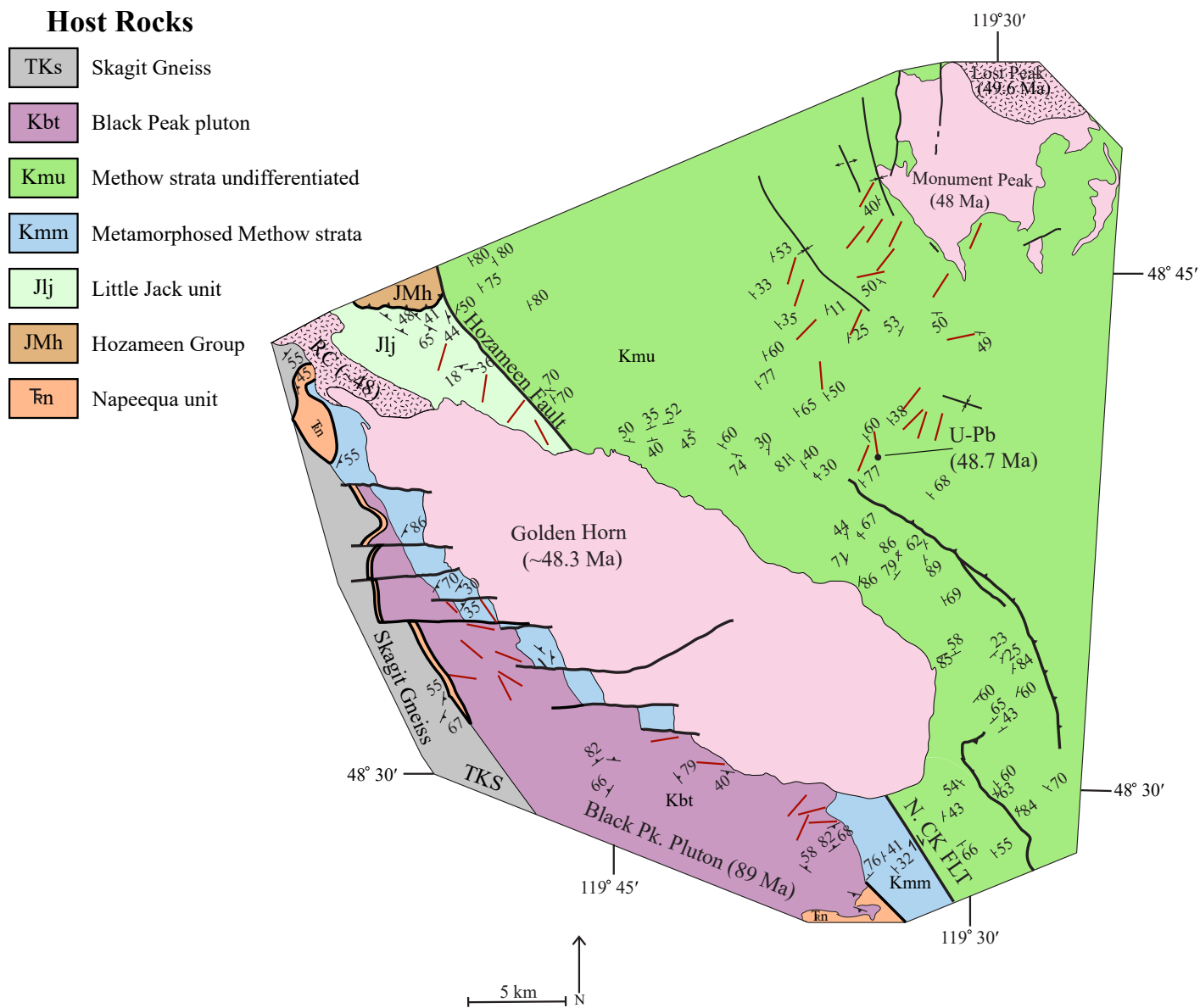
Figure 12. Map shows dike, bed, and foliation orientations and the location of the dated dike in the Golden Horn–Monument Peak domain. A few of the major fold traces and thrust faults in the Methow strata are also shown. Dikes are abundant near the Golden Horn batholith, but most of the mapped dikes are closer to the Monument Peak pluton. N. CK FLT—North Creek fault; RC—Ruby Creek plutonic belt. Modified from Stoffel and McGroder (1989), Dragovich et al. (1997), and Haugerud and Tabor (2009).

rhyolite and are more compositionally diverse than the adjacent plutons. In the Corbaley Canyon and eastern Duncan Hill domains, the diversity of dike compositions is interpreted to reflect fractional crystallization of a transitional calc-alkaline to tholeiitic parental magma (Waters, 1927; Hopson and Mattinson, 1994; Loewen et al., 2006; Davidson et al., 2015). For the eastern Duncan Hill, Cooper Mountain, and Golden Horn-Monument Peak dike domains, U-Pb zircon ages of the dikes are older than the nearby Eocene plutons. In the Corbaley Canyon domain, the ages of the dikes and the Duncan Hill pluton overlap within uncertainties, although their age relationships may become clearer with higher precision dates for the emplacement of the dikes.

Loewen et al. (2006) proposed that the dike magmas were generated by slab rollback during extension. This tectonic setting is inferred for the Eocene following the accretion of Siletzia (Schmandt and Humphreys, 2011; Tepper, 2016; Kant et al., 2018). We suggest that the dikes and plutons were generated by a common tectonic mechanism (likely slab rollback) and that the dikes represent forerunners to the more focused magmatism represented by the plutons rather than offshoots of the plutons themselves. The difference in emplacement age for many of the dikes and plutons also suggests that while they might have intruded during a common stress and strain regime, the emplacement of the plutons did not control dike orientations (see below).

Controls on Dike Orientations

Dike orientations may be controlled by regional stresses, stresses induced by magmatic centers, and structural anisotropies in dike host rocks. Tectonic rotations, such as in strike-slip shear zones, may also influence dike orientation.

Many dike swarms are interpreted to record regional strain and form perpendicular to the regional extension direction. Eocene dikes from the central Washington Cascades northward into British Columbia were largely intruded during dextral strike-slip faulting, and the regional strain field was presumably compatible with these faults. A strain field dominated by NW (~315–320°) and probably younger (post-50 Ma) N-striking (350–355°) dextral faults should result in dikes striking 005° to 040° (Fig. 2). The N-striking faults, particularly the Straight Creek fault, probably dominated during the diking and thus predict dike strikes of ~035°–040°. In transtension, dikes would intrude at a lower angle to the strike-slip faults (Fig. 2; e.g., Sanderson and Marchini, 1984) particularly when the strike-slip and extensional components are partitioned (e.g., Tikoff and Teyssier, 1994). Orogenic collapse can also lead to orogen-normal extension, and Eocene orogen-parallel flow in response to different along-strike crustal thicknesses has been proposed for the Cascades core (Paterson et al., 2004; Miller et al., 2016).

The stress field from magmatic centers (e.g., Delaney et al., 1986) may override regional stresses and control dike orientations. This effect is exemplified by radial dike swarms emanating from volcanoes and some shallow-level plutons (e.g., Muller and Pollard, 1977). Dikes may also form parallel to the contacts of some volcanoes (e.g., Chadwick and Dieterich, 1995). Many of the areas with abundant dikes in the Cascades are near Eocene plutons or postulated volcanic centers, and previous workers have suggested a direct relationship between dikes and several of these magmatic bodies (Misch, 1966; Tabor et al., 1968; Dellinger, 1996). Magma pressure from emplacement and wedging of dikes may also change the stress field by switching the orientations of principal stresses, which results in horizontal sills or an orthogonal set of vertical dikes (Parsons and Thompson, 1991; Vigneresse et al., 1999).

Anisotropies in host rocks, such as beds, faults, foliations, and joints, may control dike orientations. Some Cascades dikes intruded into or near fault zones and strike subparallel to the zones, which suggests that orientations of these dikes were influenced by fault zones. In other places, strikes are close to those of regional foliation. Joints have been studied minimally in the Cascades, and their influence is unknown.

Controls on Teanaway Dike Orientations

Previous workers suggested a close relationship between the Teanaway dikes and the Straight Creek fault, which strikes ~350–355° in the region of the dikes (e.g., Ashleman, 1979; Vance and Miller, 1983; Johnson, 1985; Miller et al., 2016). The angle between the Straight Creek fault and mean dike trend is ~41–46°, and axes of large folds in the Swauk Formation are generally at a high angle to the dikes and moderate angle (~25°–60°) to the strike of the Straight Creek fault. Axial traces rotate into sub-parallelism with the fault as it is approached, and folds become tighter and more widespread close to the fault (Foster, 1958; Ellis, 1959; Ashleman, 1979).

The eastern boundary of the Swauk Formation and Teanaway dikes is the Leavenworth fault zone, which consists of NW-striking (~320°) segments connected by shorter N-S segments (Fig. 3). In the dextral wrench fault model, dikes should strike ~005° as a result of motion on the dominant NW segments and ~045° from slip on the shorter N-S segments (although the N-S ones have an extensional component). The angle between the mean dike strike in the east (~040°; Mendoza, 2008) and the strike of the dominant segments is thus higher than predicted. These orientations are compatible with transpression but not transtension (e.g., Sanderson and Marchini, 1984; Tikoff and Teyssier, 1994). Thus, the dike orientations were unlikely to have been influenced significantly by the NW-trending segments of the Leavenworth fault, but the N-S–trending segments may have acted along with the Straight Creek fault to control dike orientations.

The Teanaway dikes were interpreted to have issued from a large volcanic center in the southwestern part of the Teanaway Formation by Clayton (1973) because the unit thickens significantly to the west. The influence of magma pressure and loading associated with this postulated volcano relative to the regional stress should decrease outward. Dikes, however, do not change much in orientation or in degree of preferred orientation with position relative to the inferred volcano (Fig. 5).

In Cenozoic mafic dike swarms in the North Atlantic (Greenland, Iceland, and British Tertiary Province), dikes increase in thickness and decrease in

number away from the presumed magmatic source probably because thinner dikes die out or merge with distance from the source (e.g., Jolly and Sanderson, 1995; Klausen, 2006; Curtis et al., 2008). For the Teanaway dikes, mean dike thicknesses decrease from 19 m in the Jolly Mountain transect (west) close to the inferred Teanaway shield volcano to ~17 m in the Koppen Mountain (west-central) transect and to ~14 m in the eastern transect (Table 3). This trend is opposite of the expected one, and thus, proximity to the volcanic source probably did not control dike thickness.

We conclude that orientations of the Teanaway dikes largely reflect the influence on the regional strain field of the Straight Creek fault and potentially the N–S segments of the Leavenworth fault. The large concentration of dikes and steepness of beds in the central part of the basin (Tabor et al., 1982, 2000) may reflect the influence there of a rigid buttress of the Mount Stuart batholith and Ingalls Complex, narrowness of the Swauk basin, and the position midway between the Straight Creek and Leavenworth faults (Fig. 5).

Controls on Corbaley Canyon Dike Orientations

The Corbaley Canyon dikes and other dikes that intruded the Cascades core lay between the dextral Ross Lake fault zone and the dextral Entiat fault, both of which strike ~315–320° (Fig. 3). Strikes of the Corbaley Canyon dikes change from mostly 100–110° east of the Columbia River to dominantly 120–140° west of the river and average ~119°, which is ~15–20° counterclockwise from the Entiat and Ross Lake faults. The average is thus ~60–65° from the expected orientation in a strain field dominated by these dextral faults and >20° for transtension (Fig. 2). The discordance is more pronounced for the N-S–striking faults (Fig. 2).

Earlier workers (Cater, 1982; Hopson et al., 1987; Dellinger, 1996) interpreted the 46.69 + 0.7/–0.73 Ma (U-Pb zircon) Corbaley Canyon domain dikes as axial dikes of the NW-trending (315–320°), 46.5 ± 0.2 Ma (U-Pb zircon) Duncan Hill pluton. We do not rule out this interpretation, but even accounting for the E-SE– to SE-side-up tilt of 10–13°, the 15–30 km along-strike distance of the dikes from the pluton and the discordance (ca. 15–20°) of the dike trends to the long axis of the pluton and to the dikes in the southern Duncan Hill domain closer to the pluton are problematic for this model. The rocks intruded by the Corbaley Canyon dikes, particularly the Napeequa unit and Swakane Gneiss, have strong foliation and are injected by concordant meter-scale sheets. These anisotropies potentially influenced dike orientations. The W-NW strike of foliation (~290° to 315°) is subparallel to the dikes, but the moderately NE dip is opposite to that of the dikes (Fig. 9) (Alsleben, 2000; Paterson et al., 2004).

Another potential influence on the strain field is the Dinkelman décollement (Figs. 3 and 9). This foliation-parallel, folded, NE-dipping detachment fault between the Swakane Gneiss and structurally overlying Napeequa unit was probably active until ca. 50–46 Ma (Paterson et al., 2004). The dikes appear to postdate the NW-trending, map-scale fold of the décollement (Paterson et al., 2004), but field relations are permissible for dike emplacement coeval with

folding, and Miller et al. (2016) noted strong ductile stretching parallel to hinge lines in the mid-crustal Skagit Gneiss Complex in the Eocene. The hinge line of the gently plunging regional antiform folding foliation and the décollement in the Corbaley Canyon domain trends ~315° (Tabor et al., 1987; Paterson et al., 2004) and is at low to moderate angles (clockwise) to the strike of the dikes rather than at the high angles predicted for transtensional folds (e.g., Fossen et al., 2013).

Sparse measurements of stretching (extension) lineations in the gneiss near the décollement in Corbaley Canyon trend ~037° and swing to 064° on the W side of the Columbia River (Alsleben, 2000; Paterson et al., 2004). Assuming that the brittle and ductile shear direction are compatible and predated the regional antiform, then extension fractures associated with movement on the décollement should strike normal to the lineation and dip at ~45° to the décollement; such fractures are predicted to strike ~307–334° and dip steeply (~75°N to 70°S). The steep dips of fractures are significantly closer to those of the dikes than are the dips of foliation, but the strikes of fractures are oblique to the strikes of dikes.

Overall, fractures associated with the décollement, or orogen-normal extension, are potentially major controls on the orientations of the Corbaley Canyon dikes. Tectonic rotation is permissible on the basis of the complex paleomagnetic data and is discussed in the next section.

Controls on Southern Duncan Hill Dikes

A dramatic, more than 60° change in dike strike occurs over a distance of ~10 km from the Corbaley Canyon domain to southern Duncan Hill domain. The NE-striking (058° maxima) southern Duncan Hill dikes record NW-SE extension subparallel to the strike of the orogen. The dike strikes are at a high (~80°) angle to the Entiat and Ross Lake faults and do not fit a wrench-dominated strain field.

The markedly different strikes (~058° versus 119° maxima) in the southern Duncan Hill and Corbaley Canyon domains (Figs. 9–10) may indicate that they formed during different events or have undergone differential vertical axis rotation. In one scenario of dextral shear and clockwise rotation, dikes intruded with a roughly constant NE strike at different times. In this model, dikes in the Corbaley Canyon domain are older than those in the southern Duncan Hill domain. There are insufficient age data to fully test this interpretation, but the rates and magnitudes of block rotation are problematic, as ≥60° of rotation would have occurred south of the Duncan Hill pluton in ca. 3 m.y. or less. These rates of ca. ≥20°/m.y. contrast with the ~5–6°/m.y. of rotation related to the San Andreas fault in southern California (e.g., Luyendyk, 1991) and the current 0.5–3.8°/m.y. of block rotation in the North Island of New Zealand (Wallace et al., 2004). If the complex, difficult to interpret paleomagnetic discordance from the Corbaley Canyon dikes described above is accounted for by ~142° of clockwise rotation (Stauss, 1982; Harrison, 1984) then the rates of rotation in the Duncan Hill region are potentially even higher. Further, local dextral or sinistral structures responsible for such rotation have not been recognized south of the Duncan Hill pluton, and orientations of host rock foliations are complex and do not obviously fit a simple rotation model.

Some of the dikes near the southern margin of the Duncan Hill pluton strike sub-parallel to the pluton contact and dip NW toward the possible roof of the pluton (Fig. 10). These dikes are not properly oriented for dikes radiating from a magmatic center, but they may have utilized fractures associated with emplacement of the pluton.

The host rocks are poorly exposed, and the few foliations shown on published maps strike E-W to NW and have generally moderate dips (Fig. 10) (Tabor et al., 1987). It thus seems unlikely that dike orientations are controlled by foliation and the dikes are not appropriately oriented for fractures associated with the Dinkelman décollement, which is nearly 20 km to the west.

We conclude that these dikes most likely record regional orogen-parallel stretching. Fractures formed by emplacement of the Duncan Hill pluton potentially played a role, although the age relationships between dikes and plutons described above do not support this interpretation.

Controls on Eastern Duncan Hill Dikes

The mean N-NE strike (025°) of dikes in the eastern Duncan Hill domain is at too high of an angle (~65–70°) to the Entiat fault and Ross Lake fault zone for a strain field dominated by these dextral strike-slip faults, and this is particularly true during transtension. The dikes are oriented similarly to the Teanaway dikes and are inferred to record regional W-NW–E-SE extension probably related to the strain field associated with the N-S–striking Straight Creek fault. The smaller but distinct NW-striking maxima of 301° is closer to the strike of the dextral faults and the orogen, but it is counter-clockwise to the faults, which does not fit with transtension. The nearly orthogonal relationship between the two sets of dikes is intriguing particularly if they are synchronous. Orthogonal vertical dikes can form in a regime where the horizontal intermediate (σ_2) and minimum (σ_3) principal stresses switch as a result of the magma overpressure induced by the emplacement of dikes (Parsons and Thompson, 1991; Vigneresse et al., 1999). Alternatively, the W-NW–striking dikes are younger than the N-NE–striking dikes, and the regional strain field changed by ~90°. Only a NE-striking dike has been dated, so more age data are needed to test this hypothesis. Arguing against this interpretation is the lack of cross-cutting dikes.

Some of the dikes may be petrogenetically related to the Duncan Hill pluton as postulated by previous workers (e.g., Hopson et al., 1987; Dellinger, 1996), but this intrusion does not appear to have been the major control on dike orientations. Mean dike strikes are at 65–70° to the trend of the Duncan Hill pluton, there is no clear relation between dike strike and the local trend of the adjacent contact of the pluton, and the average strikes of the NE- and NW-striking dikes do not change perceptibly with distance from the pluton (Fig. 10). Moreover, the U-Pb zircon age for a NE-striking porphyritic dike is ~1 m.y. older than the pluton (Tables 1–2).

Host rock foliation may have influenced the strike of the dikes. The fine-grained, thinly foliated Twentyfive Mile Creek Schist contrasts with the coarse-grained and generally weakly to moderately foliated Chelan Complex. Dikes intruding the Twentyfive Mile Creek Schist have NW (~310°) strikes within 5 km of the Duncan Hill pluton and broadly E-W (087°) strikes from 5 km to 10 km away from the pluton. These orientations are similar to those of some of the foliations in the schists, but in a number of places there is pronounced discordance (Fig. 10). The NE (average of 038°) strike of dikes intruding the Chelan Complex is discordant to foliation.

Vertical axis rotation is unlikely to explain the bimodal dike strikes. The arguments against rotation between the Corbaley Canyon domain and southern Duncan Hill domain also apply to the eastern Duncan Hill dikes. In particular, ~85° of rotation would be required in probably <3 m.y.

In summary, the NE-striking dikes are interpreted to record the regional strain field, whereas the W-NW–striking dikes may have been influenced by the anisotropy of the host Twentyfive Mile Creek Schist and/or controlled by the switch in the stress field imparted by emplacement of the NE-striking dikes. Alternatively, the NE- and W-NW–striking dikes differ in age and record a different regional strain.

Controls on Cooper Mountain Dikes

The ca. 49.3 Ma porphyritic dikes associated with the Cooper Mountain batholith intruded very shortly after the cessation of oblique (dextral-normal) motion on the NW-striking (~325°) Foggy Dew fault strand of the Ross Lake fault system, which deforms 49.3 ± 0.2 Ma orthogneiss but is cut by the ca. 49–48 Ma batholith (Miller and Bowring, 1990). The mean strike of ~010–015° of the porphyries is ~45–50° from the trend of the Foggy Dew fault zone, and the mafic dikes are at a slightly lower angle (35–40°). These strikes are compatible with those of the dextral fault zone. In contrast, the younger, poorly dated, ca. 44.5 Ma South Fork Gold Creek porphyry dikes strike NW, roughly parallel to the Foggy Dew fault zone, which they intrude (Fig. 3; Hopkins, 1987).

Orientations of the dikes do not change systematically relative to the margin of the batholith (Fig. 11) and are not likely controlled by magmatic pressure from an intrusive center. Dikes intruded subparallel to the southeastern margin may be influenced by tangential fractures that formed during intrusion of the batholith, although these dikes do not differ substantially in strike from dikes elsewhere (Fig. 11). The mean trends of the dikes are nearly perpendicular to the long axis of the Cooper Mountain batholith, which potentially indicates a genetic relationship.

The dikes are steeper than the typically moderately dipping foliation in the host rock and strike at a high angle to the widespread E-W foliations (Fig. 11). The strikes of dikes do not change where foliation swings to NE and locally NW strikes. Thus, foliation anisotropy did not control dike orientations.

Overall, the orientations of the Cooper Mountain dikes best fit regional WNW-ESE extension during dextral strike slip in the Ross Lake fault zone. The anisotropy of the fault zone may have also influenced the orientations of the South Fork Gold Creek dikes.

Controls on Golden Horn–Monument Peak Dikes

Along strike to the NW of the Cooper Mountain batholith, the ca. 48.3 Ma Golden Horn batholith truncates the Hozameen and North Creek faults of the Ross Lake fault system (Fig. 12). Mafic and felsic dikes on the S and SW sides of the Golden Horn batholith strike mostly E-W to W-NW, along with some NW strikes, which is incompatible with control by dextral faults striking ~320° (Fig. 2). Most of the N-NE to NE (mean of ~030°)–striking dikes between the NE margin of the Golden Horn batholith and the Monument Peak stock are at a higher angle than predicted for the Ross Lake fault zone but fit regional transtensional N-S strike-slip faulting (Fig. 2). The dated (U-Pb zircon) dike is also older than the pluton.

The dominant NE (030°) strike of dikes is at a high angle to the long axis of the Golden Horn batholith and the southwestern margin of the irregularly shaped Monument Peak intrusion, whereas the E-W– to W-NW–striking dikes south and west of the batholith are at low to moderate angles to the axis (Fig. 12). Influence by the magmatic centers thus cannot be ruled out but is probably not a major control.

The typical NW strike of foliation and beds in the host rocks to the Golden Horn batholith and Monument Peak stock is discordant to the strikes of dikes (Fig. 12), and foliation is weak in the plutonic host rocks. The local NW-striking dikes potentially intruded obliquely opening Mode 2 shear fractures, but no direct field evidence for this was recognized. The E-W– to W-NW–striking dikes are subparallel to steep faults that have up to 2 km of left-lateral separation of the western margin of the Golden Horn batholith (Fig. 12) (Dragovich et al., 1997; Haugerud and Tabor, 2009). Movement of these faults and the intrusion of dikes overlapped, and some dikes intruded along the faults (Dragovich et al., 1997). Thus, faults and associated fractures likely controlled some dike orientations, whereas foliation and bedding did not.

An alternative interpretation for the E-W– to W-NW–striking Golden Horn dikes is that they intruded with a NE strike and then underwent clockwise rotation. In this scenario, the E-NE– to E-W–striking faults are antithetic sinistral shears bounding rotating blocks (R′ shears; cf. Freund, 1974; Luyendyk et al., 1980; Wells et al., 2020) in the Ross Lake fault zone (Fig. 2; Haugerud et al., 1991b). The dikes would need to rotate ≥55°. Such rotation would have to occur between dike emplacement and the locking in of the paleomagnetic field in the Golden Horn batholith, which is interpreted to indicate down-to-the-N tilting about a horizontal axis by ~47 Ma (Petro et al., 2002). In contrast, if these faults are S-dipping listric or planar rotational normal faults, that could explain the tilting.

Controls on Eocene Dikes Elsewhere in the North Cascades

Controls on the orientations of less-studied areas of concentrated dikes intruding the Cascades core are poorly constrained. Dikes intruding north of the Duncan Hill pluton are mainly N-NE– to E-NE–striking, and these orientations are seen elsewhere in the Cascades. The NE strike of dikes intruding the southern part of the Skagit Gneiss Complex is broadly similar to that of several other swarms that are interpreted to record regional NW-SE extension related to N-S strike-slip faulting. The E-W–striking dikes intruding the central Skagit Gneiss Complex are subparallel to those intruding near the southern and southwestern contacts of the Golden Horn batholith ~15 km to the north. E-W–striking faults with sinistral separation offset the eastern contact of the Skagit Gneiss Complex in this area and, analogous to those faults displacing the western contact of the Golden Horn batholith, may have controlled dike orientations.

Controls on the ca. 44.9 Ma, NW-trending dikes in the northern part of the Skagit Gneiss Complex are unknown. The subhorizontal, orogen-parallel lineation in these dikes is compatible with regional dextral transtension (Haugerud et al., 1991a; Wintzer, 2012; Miller et al., 2016).

Summary of Dike Orientations and Controls of Orientations

The data presented above demonstrate a range of average orientations of dike strikes and potential controls on dike orientations for the different swarms. The strike maxima for all (n = 1118) dikes measured is 035° (Fig. 7I). This maxima excludes the voluminous Cooper Mountain dikes, which have a more northerly orientation, and the easternmost Teanaway dikes, which trend 040°. Inclusion of these dikes would result in a small, more northerly rotation of the maxima. The largest average concentration of dikes trends N–NE and includes the most voluminous dikes, and a much smaller concentration of dikes trends W–NW (~120°). The southern Duncan Hill and Hungry Mountain dikes do not fit in these clusters.

The clusters likely reflect different controls.

(1) The N-NE– to NE-striking dikes are interpreted to record regional WNW-ESE to NW-SE extension. Many of the dike orientations are compatible with the strain field that is expected for the nearby major dextral strike-slip faults and particularly the Straight Creek fault (Figs. 2 and 13).

(2) The areas of E-W– to NW-striking dikes probably result from multiple factors. Faults and associated shear fractures arguably guided the orientation of the roughly E-W– to W-NW–striking dikes S and W of the Golden Horn batholith and in the central Skagit Gneiss Complex, and the anisotropy of the Foggy Dew fault zone likely controlled the orientation of the NW-striking Hungry Mountain dikes. The Corbaley Canyon domain dikes may have intruded fractures that formed due to movement on the Dinkelman décollement. Clockwise tectonic rotation of initially NE-striking dikes to E-W to W-NW trends (Fig. 2) cannot be ruled out for the dikes on the west side of the Golden Horn batholith, but there is no direct paleomagnetic evidence for vertical axis rotation.

(3) The eastern Duncan Hill domain is the only area where both the major N-NE maxima and the subordinate W-NW concentration are developed. Regional strain during intrusion of the N-NE–striking dikes is inferred. The strong foliation in the Twentyfive Mile Creek Schist potentially
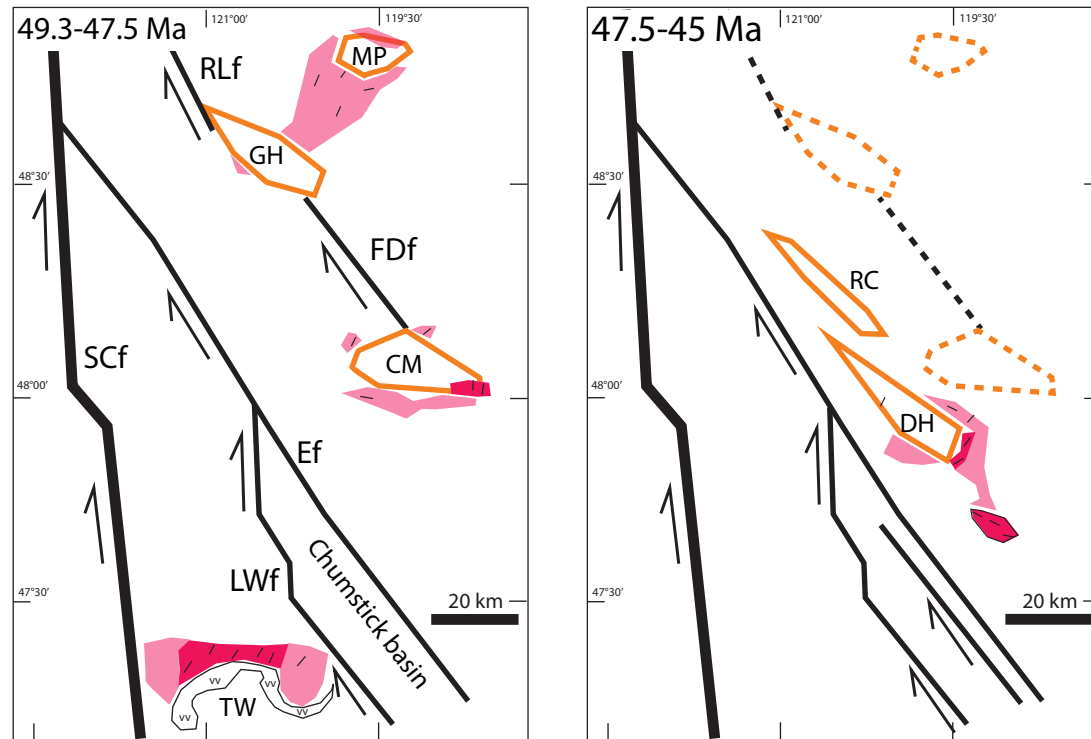
Miller et al. | Eocene dike orientations in Washington Cascades
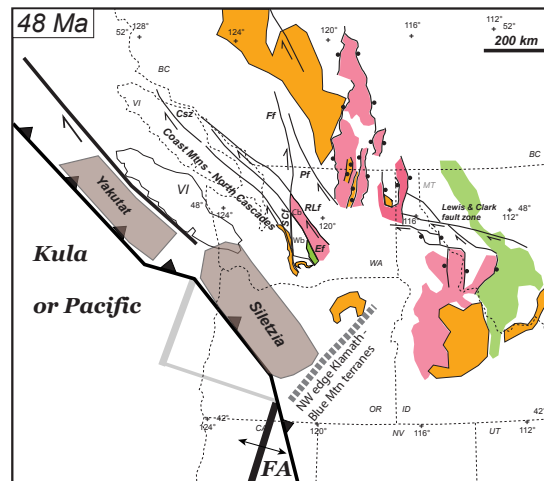
Plate Tectonic Setting

Figure 13. Summary of patterns is given for diking, plutonism, and strike-slip faulting from 49.3 Ma to 45 Ma. Some of the less-studied and less well-dated smaller areas of diking are excluded. The abundance of dikes in the top two sketch maps is indicated by the color intensity. Note that from ca. 49.3–47.5 Ma, dikes and plutons are concentrated in the vicinity of the Ross Lake (RLf) and Foggy Dew (FDf) faults of the Ross Lake fault system and at the south end of the Cascades core in the Teanaway swarm (TW). Northeast-striking dikes dominate. From 47.5 to 45 Ma, dikes and plutons lay between the Entiat fault (Ef) and now inactive Ross Lake fault system. After 45 Ma, diking and magmatism ended in the Cascades core, and the Ancestral Cascade arc initiated to the west. CM—Cooper Mountain batholith; DH—Duncan Hill pluton; GH—Golden Horn batholith; LWf—Leavenworth fault; MP—Monument Peak pluton, RC—Railroad Creek pluton; and SCf—Straight Creek fault. The plate tectonic setting at 48 Ma, near the end of the 49.3–47.5 Ma time slice, shows that Siletzia has collided, dextral strike slip is active north of the Farallon plate, and a new subduction zone is beginning to develop outboard of Siletzia. Core-complex extension to the northeast of the North Cascades core is nearing its end. Cb—Chelan block; Csz—Coast shear zone; Ef—Entiat fault; Ff—Fraser fault; FA—Farallon plate; Pf—Pasayten fault; RLf—Ross Lake fault; VI—Vancouver Island; Wb—Wenatchee block.

controlled the W-NW–striking dikes. If the nearly perpendicular concentrations are broadly coeval, then magma pressure induced from emplacement of the N-NE–striking dikes may have caused a switch in the minimum and intermediate principal stresses and resulted in the orthogonal relationship. Alternatively, a region-wide transition in the regional strain field may have occurred between intrusion of the NE-striking dikes and the W-NW–striking dikes. If so, the W-NW–striking dikes also probably record regional strain. This interpretation is briefly explored further.

Available age and orientation data do not provide a conclusive test of a temporal change in extension direction. The oldest well-dated dikes (49.272 ± 0.040 Ma) are associated with the Cooper Mountain batholith and overlap in age with the oldest indirectly dated dikes, which are the 49.3 ± 0.033 Ma Teanaway dikes. These swarms strike N–NE to NE (Fig. 13). A NE-striking Golden Horn–Monument Peak dike is 48.726 ± 0.027 Ma, and one of the NE-striking, eastern Duncan Hill dikes is 47.505 ± 0.18 Ma. In contrast, the few dated (U-Pb zircon) W-NW– to NW-striking dikes (Fig. 13) range from 46.69 +0.70/–0.73 Ma (Corbaley Canyon) to 44.857 ± 0.023 Ma (northern Skagit Gneiss Complex). The NW-striking Hungry Mountain dikes, which are only dated by K-Ar hornblende, also fall in this age cluster. One interpretation of these data is that the regional strain field changed between ca. 47.5 Ma and 46.7 Ma; however, the small W-NW–striking maxima of the eastern Duncan Hill dikes has not been dated, and cross-cutting relations between NE- and W-NW–striking dikes have not been recognized.

There are a few other changes in the regional tectonics at ca. 47 Ma, which include the end of major magmatism and strike-slip in the region of the Ross Lake fault zone by ca. 48 Ma and the westward migration of plutonism to the markedly elongate, 46.5 Ma Duncan Hill pluton and 45.5 Ma Railroad Creek pluton (Figs. 3 and 13). Similarly, the well-dated 49.3–48.7 Ma dikes intruded the Ross Lake fault zone and the Methow basin to the NE and the area directly south of the Cascades core, whereas the well-dated younger dikes intruded between the Ross Lake fault zone and the Entiat fault (Fig. 13). Exhumation of the Skagit Gneiss Complex probably initiated, or began in earnest, at ca. 47 Ma (Wernicke and Getty, 1997; Gordon et al., 2010; Miller et al., 2016). Reorganization of the Eocene Chumstick basin also occurred at ca. 46–45 Ma (Eddy et al., 2016a). More high-precision dating is necessary to test these hypotheses.

If the regional strain field is the major control on dike orientation, then we can speculate about the processes that were responsible for the strain field. The voluminous NE-striking dikes, dextral strike-slip faults, basins, and sub-horizontal stretching lineations in crystalline rocks record a large transtensional and magmatic event along with the voluminous Cooper Mountain batholith and Golden Horn batholith. This event occurred during or almost immediately after accretion of Siletzia and rollback and break-off of the Farallon slab (Schmandt and Humphreys, 2011). Following accretion of Siletzia, workers have speculated that part of the Pacific Northwest and southern British Columbia margin of North America was juxtaposed with the Kula or Resurrection plate (Figs. 1 and 13) (e.g., Wells et al., 1984; Haeussler et al., 2003a; Madsen et al.,

2006; Eddy et al., 2016a). This geometry can explain the acceleration of right lateral, strike-slip faulting at ca. 49 Ma resulting from the more oblique motion of the Kula or Resurrection plate relative to North America compared with that of the Farallon plate.

Diking ended in the Cascades core at ca. 45 Ma, and by 45–44 Ma basaltic and andesitic magmas erupted west of the Cascades core to form a N-S–striking magmatic arc (ancestral Cascadia arc) (Fig. 1C) that is associated with a new subduction zone outboard of Siletzia (e.g., Schmandt and Humphreys, 2011; Dragovich et al., 2016; Kant et al., 2018). The elongate Oligocene and Miocene plutons of this arc trend N-S (Haugerud and Tabor, 2009) in contrast to the NW trends of the ≥45 Ma, elongate plutons in the Cascades core.

The relatively short-lived (ca. 4 Ma), intense episode of diking and plutonism in the Cascades core occurred during rapid evolution of the plate boundary between ca. 49 Ma and 45 Ma. The transition from nearly solely NE-striking dikes intruded between 49.3 Ma to 47.5 Ma to both NE-striking and NW-striking dikes during this interval of plate reorganization speculatively reflects the development of a new regional strain field. In short, we contend that the Cascades dikes provide important "snapshots" of the regional strain field and tectonics.

■ CONCLUSIONS

Eocene dikes ranging from ca. 49.3 Ma to 44.9 Ma intruded a large region in the central and northern Washington Cascades during the transition from collision of Siletzia, rollback of the Farallon slab, and passage of a triple junction to the establishment of a new plate boundary. Intrusion of the oldest (ca. 49.3–47.5 Ma) and greatest number of dikes coincided with an increase in dextral strike-slip faulting, mafic volcanism, and silicic plutonism. Mean dike trends (~035°) indicate WNW-ESE to NW-SE extension, which is broadly compatible with the strain field expected for the major dextral N-S–striking Straight Creek fault and to a lesser extent the NW-striking Ross Lake fault and Entiat fault. The much smaller maxima of dike strikes is ca. 300°; at least some of these dikes are younger than 47 Ma and temporally overlap with intrusion of the youngest Eocene plutons in the North Cascades. Pre-existing structural anisotropies, including strong host-rock foliations, tension fractures related to the Eocene Dinkelman décollement, and faults arguably controlled orientations of the W-NW–striking dikes and a small concentration of ~E-W–striking dikes. Alternatively, these dikes may reflect a switch in the regional strain field to NNE-SSW extension between ca. 47.5 Ma and 46.7 Ma. Magmatic centers had no obvious influence on dike orientations, although magmatic pressure by dikes may have changed the principal stress axes in one domain and led to orthogonal sets of dikes. Paleomagnetic data imply that vertical axis rotation during dextral strike slip is unlikely to explain contrasting dike orientations.

Magmatic extensions determined from well-exposed transects through many of the swarms range from ~5% to locally ~79% and correspond to

~12 km of extension. This is a minimum value, as extension from intrusion of several swarms has not been calculated.

Diking and transtension in the Cascades overlap temporally with magmatism, metamorphic core complex formation, and non-marine sedimentation to the E and NE, where extension is closer to E-W than the WNW-ESE extension of the coeval N-NE–striking dikes in the Cascades. This difference probably represents the effects of dextral strike-slip along the plate boundary in response to the passage of the triple junction and the influence of the Kula or Resurrection plate. The shutoff of diking resulted from the jump of the subduction zone outboard of Siletzia and associated westward migration of magmatism with the initiation of the ancestral N-S–trending Cascade arc. This study illustrates the importance of dikes in recording regional strain at the orogen scale and the potential role of multiple controls on dike orientations during regional transtension and ridge-trench interaction.

REFERENCES CITED

Alsleben, H., 2000, Structural analysis of the Swakane terrane, North Cascades core, Washington [M.S. thesis]: San Jose, California, USA, San Jose State University, 168 p.

Anderson, E.M., 1951, The Dynamics of Faulting and Dyke Formation with Applications to Britain: Edinburgh, UK, Oliver and Boyd, 206 p.

Ashleman, J.C., 1979, The geology of the western part of the Kachess Lake quadrangle, Washington, USA [M.S. thesis]: Seattle, Washington, USA, University of Washington, 88 p.

Barksdale, J.D., 1975, Geology of the Methow Valley, Okanogan County, Washington: State of Washington Department of Natural Resources, Division of Geology and Earth Resources Bulletin 68, 72 p.

Bartley, J.M., Glazner, A.F., Coleman, D.S., Kylander-Clark, A.R.C., and Maples, R., 2007, Large Laramide dextral offsets across Owens Valley, California, and its possible relation to tectonic unroofing of the southern Sierra Nevada, in Till, A.B., Roeske, S.M., Sample, J.C., and Foster, D.A., eds., Exhumation Associated with Continental Strike-Slip Fault Systems: Geological Society of America Special Paper 434, p. 129–148, https://doi.org/10.1130/2007.2434(07).

Beck, M.E., Burmester, R.F., and Schoonover, R., 1982, Tertiary paleomagnetism of the north Cascade Range, Washington: Geophysical Research Letters, v. 9, p. 515–518, https://doi.org/10.1029/GL009i005p00515.

Beske, S.J., Beck, M.E., and Noson, L., 1973, Paleomagnetism of the Miocene Grotto and Snoqualmie batholiths, central Cascades, Washington: Journal of Geophysical Research, v. 78, p. 2601–2608, https://doi.org/10.1029/JB078i014p02601.

Breitsprecher, K., Thorkelson, D.J., Groome, W.G., and Dostal, J., 2003, Geochemical confirmation of the Kula-Farallon slab window beneath the Pacific Northwest in Eocene time: Geology, v. 31, p. 351–354, https://doi.org/10.1130/0091-7613(2003)031<0351:GCOTKF>2.0.CO;2.

Brown, E.H., 1987, Structural geology and accretionary history of the Northwest Cascades system, Washington and British Columbia: Geological Society of America Bulletin, v. 99, p. 201–214, https://doi.org/10.1130/0016-7606(1987)99<201:SGAAHO>2.0.CO;2.

Bryant, K., 2017, Structural analysis of Eocene dike swarms in and near the Duncan Hill pluton, North Cascades, Washington [M.S. thesis]: San Jose, California, USA, San Jose State University, 61 p.

Cater, F.W., 1982, Intrusive rocks of the Holden and Lucerne quadrangles, Washington; the relation of depth zones, composition, textures, and emplacement of plutons: U.S. Geological Survey Professional Paper 1220, 108 p., https://doi.org/10.3133/pp1220.

Cater, F.W., and Crowder, D.F., 1967, Geologic map of the Holden quadrangle, Snohomish and Chelan Counties, Washington: U.S. Geological Survey Map GQ-646, scale 1:62,500, 1 sheet.

Cater, F.W., and Wright, T.L., 1967, Geologic map of the Lucerne quadrangle, Chelan County, Washington: U.S. Geological Survey Map GQ-647, scale 1:62,500, 1 sheet.

Chadwick, W.W., and Dieterich, J.H., 1995, Mechanical modeling of circumferential and radial dike intrusion on Galapagos volcanoes: Journal of Volcanology and Geothermal Research, v. 66, p. 37–52, https://doi.org/10.1016/0377-0273(94)00060-T.

Cheney, E.S., and Hayman, N.W., 2009, The Chiwaukum structural low: Cenozoic shortening of the central Cascade Range, Washington State, USA: Geological Society of America Bulletin, v. 121, p. 1135–1153, https://doi.org/10.1130/B26446.1.

Clark, K.P., 1989, The stratigraphy and geochemistry of the Crescent Formation basalts and the bedrock geology of associated igneous rocks near Bremerton Washington [M.S. thesis]: Bellingham, Washington, USA, Western Washington University, 171 p.

Clayton, D.N., 1973, Volcanic history of the Teanaway Basalt, east-central Cascade Mountains, Washington [M.S. thesis]: Seattle, Washington, USA, University of Washington, 55 p.

Curtis, M.L., Teal, R.R., Owens, W.H., Leat, P.T., and Duncan, R.A., 2008, The form, distribution and anisotropy of magnetic susceptibility of Jurassic dykes in H.U. Sverdrupfjella, Dronning Maud Land, Antarctica. Implications for dyke swarm emplacement: Journal of Structural Geology, v. 30, p. 1429–1447, https://doi.org/10.1016/j.jsg.2008.08.004.

Davidson, P., Tepper, J.H., and Nelson, B.K., 2015, Petrology of Eocene dikes near Lake Chelan, WA: Evidence of mantle and crustal melting during the Challis event: Abstract V23B–3121 presented at 2015 Fall Meeting, American Geophysical Union, San Francisco, California, USA, 14–18 December.

Delaney, P., and Pollard, D.D., 1981, Deformation of host rock and flow of mafic magma during growth of minette dikes and breccia-bearing intrusions near Ship Rock, New Mexico: U.S. Geological Survey Professional Paper 1202, 61 p.

Delaney, P.T., Pollard, D.D., Ziony, J.I., and McKee, E.H., 1986, Field relations between dikes and joints: Emplacement processes and paleostress analysis: Journal of Geophysical Research: Solid Earth, v. 91, p. 4920–4938, https://doi.org/10.1029/JB091iB05p04920.

Dellinger, D.A., 1996, The geology, petrology, geochemistry, mineralogy, and diapiric emplacement of the Duncan Hill pluton [Ph.D. thesis]: Santa Barbara, California, USA, University of California, 538 p.

Dickinson, W.R., and Snyder, W.S., 1979, Geometry of subducted slabs related to San Andreas transform: The Journal of Geology, v. 87, p. 609–627, https://doi.org/10.1086/628456.

Donaghy, E.E., Umhoefer, P.J., Eddy, M.P., Miller, R.B., and LaCasse, L., 2021, Stratigraphy, age, and provenance of the Eocene Chumstick Basin, Washington Cascades; implications for paleogeography and regional tectonics: Geological Society of America Bulletin, v. 133, p. 2418–2438, https://doi.org/10.1130/B35738.1.

Doran, B.A., 2009, Structure of the Swauk Formation and Teanaway dike swarm, Washington Cascades [M.S. thesis]: San Jose, California, USA, San Jose State University, 97 p.

Dragovich, J.D., Norman, D.K., Haugerud, R.A., and Miller, R.B., 1997, Geologic map of the Gilbert 7.5 minute quadrangle, Chelan and Okanogan Counties, Washington: Washington Division of Geology and Earth Resources Map GM-46, scale 1:24,000, 1 sheet, 67 p. text.

Dragovich, J.D., Mavor, S.P., Anderson, M.L., Mahan, S.A., MacDonald, J.H., Jr., Tepper, J.H., Smith, D.T., Stoker, B.A., Koger, C.J., Cakir, R., DuFrane, S.A., Scott, S.P., and Justman, B.P., 2016, Geologic map of the Granite Falls 7.5 minute Quadrangle, Snohomish County, Washington: Washington Division of Geology and Earth Resources, Geologic Map Series, 2016–03.

Eddy, M.P., Bowring, S.A., Umhoefer, P.J., Miller, R.B., McLean, N.M., and Donaghy, E.E., 2016a, High-resolution temporal and stratigraphic record of microplate accretion and ridge-trench interaction preserved in non-marine sedimentary basins in central and western Washington: Geological Society of America Bulletin, v. 128, p. 425–441, https://doi.org/10.1130/B31335.1.

Eddy, M.P., Bowring, S.A., Miller, R.B., and Tepper, J.H., 2016b, Rapid assembly and crystallization of a fossil large-volume silicic magma chamber: Geology, v. 44, p. 331–334, https://doi.org/10.1130/G37631.1.

Eddy, M.P., Clark, K.P., and Polenz, M., 2017a, Age and volcanic stratigraphy of the Eocene Siletzia oceanic plateau in Washington and on Vancouver Island: Lithosphere, v. 9, p. 652–664, https://doi.org/10.1130/L650.1.

Eddy, M.P., Umhoefer, P.J., Miller, R.B., Donaghy, E.E., Gundersen, M., and Senes, F.I., 2017b, Sedimentary, volcanic, and structural processes during triple-junction migration: Insights from

the Paleogene record in central Washington, *in* Haugerud, R.A., and Kelsey, H.M., eds., From the Puget Lowland to East of the Cascade Range: Geologic Excursions in the Pacific Northwest: Geological Society of America Field Guide 49, p. 143–173, https://doi.org/10.1130/2017.0049(07).

Ellis, R.C., 1959, The geology of the Dutch Miller Gap area [Ph.D. thesis]: Seattle, Washington, USA, University of Washington, 112 p.

Ernst, R.E., Head, J.W., Parfitt, E., Grosfils, E., and Wilson, L., 1995, Giant radiating dyke swarms on Earth and Venus: Earth-Science Reviews, v. 39, p. 1–58, https://doi.org/10.1016/0012-8252(95)00017-5.

Evans, J.E., 1994, Depositional history of the Eocene Chumstick Formation: Implications of tectonic partitioning for the history of the Leavenworth and Entiat-Eagle Creek fault systems, Washington: Tectonics, v. 13, p. 1425–1444, https://doi.org/10.1029/94TC01321.

Ewing, T., 1980, Paleogene tectonic evolution of the Pacific Northwest: The Journal of Geology, v. 88, p. 619–638, https://doi.org/10.1086/628551.

Fawcett, T.C., Burmester, R.F., Housen, B.A., and Iriondo, A., 2003, Tectonic implications of magnetic fabrics and remanence in the Cooper Mountain pluton, North Cascade Mountains, Washington: Canadian Journal of Earth Sciences, v. 40, p. 1335–1356, https://doi.org/10.1139/e03-055.

Fossen, H., Teyssier, C., and Whitney, D.L., 2013, Transtensional folding: Journal of Structural Geology, v. 56, p. 89–102, https://doi.org/10.1016/j.jsg.2013.09.004.

Foster, R.J., 1958, The Teanaway dike swarm of Central Washington: American Journal of Science, v. 256, p. 644–653, https://doi.org/10.2475/ajs.256.9.644.

Freund, R., 1974, Kinematics of transform and transcurrent faults: Tectonophysics, v. 21, p. 93–134, https://doi.org/10.1016/0040-1951(74)90064-X.

Gans, P.B., and Gentry, B.J., 2016, Dike emplacement, footwall rotation, and the transition from magmatic to tectonic extension in the Whipple Mountains metamorphic core complex, southeastern California: Tectonics, v. 35, p. 2564–2608, https://doi.org/10.1002/2016TC004215.

Glazner, A.F., Bartley, J.M., and Carl, B.S., 1999, Oblique opening and noncoaxial emplacement of the Jurassic Independence dike swarm, California: Journal of Structural Geology, v. 21, p. 1275–1283, https://doi.org/10.1016/S0191-8141(99)00090-5.

Gordon, S.M., Whitney, D.L., Miller, R.B., McLean, N., and Seaton, N.C.A., 2010, Metamorphism and deformation at different structural levels in a strike-slip fault zone, Ross Lake fault, North Cascades, USA: Journal of Metamorphic Geology, v. 28, p. 117–136, https://doi.org/10.1111/j.1525-1314.2009.00860.x.

Gresens, R.L., Naeser, C.W., and Whetten, J.T., 1981, Stratigraphy and age of the Chumstick and Wenatchee formations; Tertiary fluvial and lacustrine rocks, Chiwaukum Graben, Washington: Geological Society of America Bulletin, Part II, v. 92, p. 223–236, https://doi.org/10.1130/GSAB-P2-92-841.

Groome, W.G., Thorkelson, D.J., Friedman, R.M., Mortensen, J.M., Massey, N.W.D., Marshall, D.D., and Layer, P.W., 2003, Magmatic and tectonic history of the Leech River Complex, Vancouver Island, British Columbia: Evidence for ridge-trench intersection and accretion of the Crescent Terrane, *in* Sisson, V.B., Roeske, S.M., and Pavlis, T.L., eds., Geology of a Transpressional Orogen Developed during Ridge-Trench Interaction along the North Pacific Margin: Geological Society of America Special Paper 371, p. 327–353, https://doi.org/10.1130/0-8137-2371-X.327.

Gudmundsson, A., 1990, Dyke emplacement at divergent plate boundaries, *in* Parker, A.J., Rickwood, P.C., and Tucker, D.H., eds., Mafic Dykes and Emplacement Mechanisms: Rotterdam, The Netherlands, Balkeema, p. 47–62.

Gudmundsson, A., 1995, The geometry and growth of dykes, *in* Baer, G., and Heimann, A., eds., The Physics and Chemistry of Dykes: Rotterdam, The Netherlands, Balkema, p. 23–34.

Gudmundsson, A., 2011, Deflection of dykes into sills at discontinuities and magma-chamber formation: Tectonophysics, v. 500, p. 50–64, https://doi.org/10.1016/j.tecto.2009.10.015.

Gundersen, M., 2017, A record of the evolving Eocene tectonics of the Pacific Northwest in the Swauk Formation, central Washington [M.S. thesis]: Flagstaff, Arizona, USA, Northern Arizona University, 202 p.

Haeussler, P.J., Bradley, D.C., Wells, R.E., and Miller, M.L., 2003a, Life and death of the Resurrection plate: Evidence for its existence and subduction in the northeastern Pacific in Paleocene–Eocene time: Geological Society of America Bulletin, v. 115, p. 867–880, https://doi.org/10.1130/0016-7606(2003)115<0867:LADOTR>2.0.CO;2.

Haeussler, P.J., Bradley, D.C., and Goldfarb, R.J., 2003b, Brittle deformation along the Gulf of Alaska margin in response to Paleogene-Eocene triple junction migration, *in* Sisson, V.B., Roeske, S.M., and Pavlis, T.L., eds., Geology of a Transpressional Orogen Developed during Ridge-Trench Interaction along the North Pacific Margin: Geological Society of America Special Paper 371, p. 119–140, https://doi.org/10.1130/0-8137-2371-X.119.

Harrison, W.J., 1984, Paleomagnetism of four Late Cretaceous plutons North Cascades, Washington [M.S. thesis]: Bellingham, Washington, USA, Western Washington University, 106 p.

Haugerud, R.A., and Tabor, R.W., 2009, Geologic map of the North Cascade Range, Washington: U.S. Geological Survey Scientific Investigations Map 2940, 2 sheets, scale 1:200,000, 2 pamphlets, 29 p. text and 23 p. text.

Haugerud, R.A., van der Heyden, P., Tabor, R.W., Stacey, J.S., and Zartman, R.E., 1991a, Late Cretaceous and early Tertiary plutonism and deformation in the Skagit Gneiss Complex, North Cascade Range, Washington and British Columbia: Geological Society of America Bulletin, v. 103, p. 1297–1307, https://doi.org/10.1130/0016-7606(1991)103<1297:LCAETP>2.3.CO;2.

Haugerud, R.A., Miller, R.B., Tabor, R.W., and Phillips, W.M., 1991b, Ross Lake fault near Gabriel Peak, North Cascades Range, Washington: Geological Society of America Abstracts with Programs, v. 23, no. 2, p. 34.

Hiess, J., Condon, D.J., McLean, N.M., and Noble, S.R., 2012, ^{238}U/^{235}U systematics in terrestrial Uranium-bearing minerals: Science, v. 335, p. 1610–1614, https://doi.org/10.1126/science.1215507.

Hopkins, W.N., 1987, Geology of the Newby Group and adjacent units in the southern Methow trough, northeast Cascades, Washington [M.S. thesis]: San Jose, California, USA, San Jose State University, 95 p.

Hopson, C.A., and Mattinson, J.M., 1994, Chelan Migmatite Complex, Washington: Field evidence for mafic magmatism, crustal anatexis, mixing and protodiapiric emplacement, *in* Swanson, D.A., and Haugerud, R.A., eds., Geologic Field Trips in the Pacific Northwest: Seattle, Washington, USA, Department of Geological Sciences, University of Washington, published in conjunction with the Annual Meeting of the Geological Society of America, Seattle, Washington, 24–27 October 1994, p. 1–21.

Hopson, C.A., Dellinger, D.A., and Mattinson, J.M., 1987, Crust, mantle, and hybrid components of a 4-dimensionally zoned granitoid pluton, North Cascades, Washington: Eos (Transactions, American Geophysical Union), v. 68, no. 44, p. 1513.

Jaffey, A.H., Flynn, K.F., Glendenin, L.E., Bentley, W.C., and Essling, A.M., 1971, Precision measurement of half-lives and specific activities of ^{235}U and ^{238}U: Physical Review C, v. 4, p. 1889–1906, https://doi.org/10.1103/PhysRevC.4.1889.

Johnson, S.Y., 1985, Eocene strike-slip faulting and nonmarine basin formation in Washington, *in* Biddle, K.T., and Christie-Blick, N., eds., Strike-Slip Deformation, Basin Formation, and Sedimentation: Society of Economic Paleontologists and Mineralogists Special Publication, no. 37, p. 283–302, https://doi.org/10.2110/pec.85.37.0283.

Johnston, S.T., and Acton, S., 2003, The Eocene Southern Vancouver Island Orocline—A response to seamount accretion and the cause of fold-and-thrust belt and extensional basin formation: Tectonophysics, v. 365, p. 165–183, https://doi.org/10.1016/S0040-1951(03)00021-0.

Jolly, R.J.H., and Sanderson, D.J., 1995, Variation in the form and distribution of dykes in the Mull swarm, Scotland: Journal of Structural Geology, v. 17, p. 1543–1557, https://doi.org/10.1016/0191-8141(95)00046-G.

Jourdan, F., Feraud, G., Bertrand, H., Watkeys, M.K., Kampunzu, A.B., and Le Gall, B., 2006, Basement control on dyke distribution in large igneous provinces: Case study of the Karoo triple junction: Earth and Planetary Science Letters, v. 241, p. 307–322, https://doi.org/10.1016/j.epsl.2005.10.003.

Kant, L.B., Tepper, J.H., Eddy, M.P., and Nelson, B.K., 2018, Eocene Basalt of Summit Creek: Slab breakoff magmatism in the central Washington Cascades, USA: Lithosphere, v. 10, p. 792–805, https://doi.org/10.1130/L731.1.

Klausen, M.B., 2006, Similar dyke thickness variation across three volcanic rifts in the North Atlantic region: Implications for intrusion mechanisms: Lithosphere, v. 92, p. 137–153.

Kruckenberg, S.C., Whitney, D.L., Teyssier, C., Fanning, C.M., and Dunlap, W.J., 2008, Paleocene-Eocene migmatite crystallization, extension, and exhumation in the hinterland of the northern Cordillera: Okanogan dome, Washington, USA: Geological Society of America Bulletin, v. 120, p. 912–929, https://doi.org/10.1130/B26153.1.

Loewen, M., Brown, M., Cohen, J., Manthei, C.D., Eiriksson, D., Johnson, B., Phelps, D., and Tepper, J.H., 2006, Petrology of Eocene dike swarm in Corbaley Canyon, central Cascades, Washington: Geological Society of America Abstracts with Programs, v. 38, no. 5, p. 95.

Luyendyk, B.P., 1991, A model for Neogene crustal rotations, transtension, and transpression in southern California: Geological Society of America Bulletin, v. 103, p. 1528–1536, https://doi.org/10.1130/0016-7606(1991)103<1528:AMFNCR>2.3.CO;2.

Luyendyk, B.P., Kamerling, M.J., and Terres, R., 1980, Geometric model for Neogene crustal rotations in southern California: Geological Society of America Bulletin, v. 91, p. 211–217, https://doi.org/10.1130/0016-7606(1980)91<211:GMFNCR>2.0.CO;2.

Madsen, J.K., Thorkelson, D.J., Friedman, R.M., and Marshall, D.D., 2006, Cenozoic to Recent plate configurations in the Pacific Basin: Ridge subduction and slab window magmatism in western North America: Geosphere, v. 2, p. 11–34, https://doi.org/10.1130/GES00020.1.

Miller et al. | Eocene dike orientations in Washington Cascades

Martínez-Posa, A.I., Druguet, E., Castano, L.M., and Carreras, J., 2014, Dyke intrusion into a pre-exiting joint network: The Aiguablava lamrophyre dyke swarm (Catalan Coastal Ranges): Tectonophysics, v. 630, p. 75–90, https://doi.org/10.1016/j.tecto.2014.05.015.

Massey, N.W.D., 1986, Metchosin Igneous Complex, southern Vancouver Island: Ophiolite stratigraphy developed in an emergent island setting: Geology, v. 14, p. 602–605, https://doi.org/10.1130/0091-7613(1986)14<602:MICSVI>2.0.CO;2.

Matzel, J.E.P., 2004, Rates of tectonic and magmatic processes in the North Cascades continental magmatic arc [Ph.D. thesis]: Cambridge, Massachusetts, USA, Massachusetts Institute of Technology, 249 p.

McCrory, P.A., and Wilson, D.S., 2013, A kinematic model for the formation of the Siletz-Crescent forearc terrane by capture of coherent fragments of the Farallon and Resurrection plates: Tectonics, v. 32, p. 718–736, https://doi.org/10.1002/tect.20045.

McGroder, M.F., 1991, Reconciliation of two-sided thrusting, spatial metamorphism, and diachronous uplift in the Cascades of Washington and British Columbia: Geological Society of America Bulletin, v. 103, p. 189–209, https://doi.org/10.1130/0016-7606(1991)103<0189:ROTSTB>2.3.CO;2.

Mendoza, M., 2008, Tectonic implications of Eocene Teanaway dike swarm in the eastern Swauk basin, central Washington: Geological Society of America Abstracts with Programs, v. 40, no. 1, p. 66.

Michels, Z.D., 2008, Structure of the central Skagit Gneiss Complex, North Cascades, Washington [M.S. thesis]: San Jose, California, USA, San Jose State University, 95 p.

Miller, J.S., Matzel, J.E.P., Miller, C.F., Burgess, S.D., and Miller, R.B., 2007, Zircon growth and recycling during the assembly of large, composite arc plutons: Journal of Volcanology and Geothermal Research, v. 167, p. 282–299, https://doi.org/10.1016/j.jvolgeores.2007.04.019.

Miller, R.B., and Bowring, S.A., 1990, Structure and chronology of the Oval Peak batholith and adjacent rocks: Implications for the Ross Lake fault zone, North Cascades, Washington: Geological Society of America Bulletin, v. 102, p. 1361–1377, https://doi.org/10.1130/0016-7606(1990)102<1361:SACOTO>2.3.CO;2.

Miller, R.B., Gordon, S.M., Bowring, S.A., Doran, B.A., Michels, Z., Shea, E.K., and Whitney, D.L., 2016, Linking deep and shallow crustal processes during regional transtension in an exhumed continental arc, North Cascades, northwestern Cordillera (USA): Geosphere, v. 12, p. 900–924, https://doi.org/10.1130/GES01262.1.

Misch, P., 1966, Tectonic evolution of the northern Cascades of Washington State—A west Cordilleran case history: Canadian Institute of Mining and Metallurgy, Special Publication, v. 8, p. 101–148.

Misch, P., 1967, Plagioclase compositions and non-anatectic origin of migmatitic gneisses in Northern Cascade Mountains of Washington State: Contributions to Mineralogy and Petrology, v. 17, p. 1–70, https://doi.org/10.1007/BF00371809.

Misch, P., 1977a, Dextral displacements at some major strike faults in the North Cascades: Geological Association of Canada Abstracts with Programs, v. 2, p. 37.

Misch, P., 1977b, Bedrock geology of the North Cascades, in Brown, E.H., and Ellis, R.C., eds., Geological Excursions in the Pacific Northwest: Bellingham, Washington, USA, Western Washington University Publication, p. 1–63.

Monger, J.W.H., 1986, Geology between Harrison Lake and Fraser River, Hope map area, southwestern British Columbia, in Current Research, Part B: Geological Survey of Canada Paper 86–1B, p. 699–706.

Monger, J.W.H., and Brown, E.H., 2016, Tectonic evolution of the southern Coast-Cascade orogen, in Cheney, E.S., ed., The Geology of Washington and Beyond: From Laurentia to Cascadia: Seattle, Washington, USA, University of Washington Press, p. 101–130.

Muller, O.H., and Pollard, D.D., 1977, The stress state near Spanish Peaks, Colorado determined from a dike pattern: Pure and Applied Geophysics, v. 115, p. 69–86, https://doi.org/10.1007/BF01637098.

Parrish, R.R., Carr, S.D., and Parkinson, D.L., 1988, Eocene extensional tectonics and geochronology of the southern Omineca Belt, British Columbia and Washington: Tectonics, v. 7, p. 181–212, https://doi.org/10.1029/TC007i002p00181.

Parsons, T., and Thompson, G., 1991, The role of magma overpressure in suppressing earthquakes and topography: Worldwide examples: Science, v. 253, p. 1399–1402, https://doi.org/10.1126/science.253.5026.1399.

Paterson, S.R., Miller, R.B., Alsleben, H., Whitney, D.L., Valley, P.M., and Hurlow, H., 2004, Driving mechanisms for >40 km of exhumation during contraction and extension in a continental arc, Cascades core, Washington: Tectonics, v. 23, TC3005, https://doi.org/10.1029/2002TC001440.

Pearson, R.C., and Obradovich, J.D., 1977, Eocene rocks in northeast Washington—Radiometric ages and correlation: U.S. Geological Survey Bulletin 1433, 41 p.

Peters, R.L., and Tepper, J.H., 2006, Petrology of the Teanaway dike swarm, central Cascades, Washington: Geological Society of America Abstracts with Programs, v. 38, no. 5, p. 9.

Petro, G.T., Housen, B.A., and Iriondo, A., 2002, Tectonic significance of paleomagnetism of the Eocene Golden Horn batholith: Geological Society of America, Abstracts with Programs, v. 34, no. 5, p. A-96.

Raviola, F.P., 1988, Metamorphism, plutonism and deformation in the Pateros-Alta Lake region, north-central Washington [M.S. thesis]: San Jose, California, USA, San Jose State University, 181 p.

Samperton, K.M., Schoene, B., Cottle, J.M., Keller, C.B., Crowley, J.L., and Schmitz, M.D., 2015, Magma emplacement differentiation and cooling in the middle crust: Integrated zircon geochronological-geochemical constraints from the Bergell intrusion, Central Alps: Chemical Geology, v. 417, p. 322–340, https://doi.org/10.1016/j.chemgeo.2015.10.024.

Sanderson, D.J., and Marchini, W.R., 1984, Transpression: Journal of Structural Geology, v. 6, p. 449–458, https://doi.org/10.1016/0191-8141(84)90058-0.

Schmandt, B., and Humphreys, E., 2011, Seismically imaged relict slab from the 55 Ma Siletzia accretion to the northwest United States: Geology, v. 39, p. 175–178, https://doi.org/10.1130/G31558.1.

Scudder, C., 2018, Structure and emplacement of the Eocene Golden Horn batholith, North Cascades, Washington [M.S. thesis]: San Jose, California, USA, San Jose State University, 58 p.

Shea, E.K., 2008, Structure of the southern Skagit Gneiss Complex, North Cascades, Washington [M.S. thesis]: San Jose, California, USA, San Jose State University, 90 p.

Sisson, V.B., Roeske, S.M., and Palvis, T.L., 2003, Introduction: An overview of ridge-trench interactions in modern and ancient settings, in Sisson, V.B., Roeske, S.M., and Palvis, T.L., eds., Geology of a Transpressional Orogen Developed during Ridge-Trench Interaction along the North Pacific Margin: Geological Society of America Special Paper 371, p. 1–18, https://doi.org/10.1130/0-8137-2371-X.1.

Smith, G.O., 1904, Description of the Mount Stuart quadrangle, Washington: Washington, D.C., U.S. Geological Survey, Geologic Atlas, Folio 106, 10 p.

Stauss, L.D., 1982, Anomalous paleomagnetic directions in Eocene dikes of central Washington [M.S. thesis]: Bellingham, Washington, USA, Western Washington University, 101 p.

Stelten, M.E., Cooper, K.M., Vazquez, J.A., Calvert, A.T., and Glessner, J.J.G., 2015, Mechanisms and timescales of generating eruptible rhyolitic magmas at Yellowstone caldera from zircon and sanidine geochronology and geochemistry: Journal of Petrology, v. 56, p. 1607–1642, https://doi.org/10.1093/petrology/egv047.

Stoffel, K.L., and McGroder, M.F., 1989, Geologic map of the Robinson Mountain 1:100,000-scale quadrangle, Washington: Washington Division of Geology and Earth Resources Open-File Report 90–5, 39 p.

Stoffel, K.L., Joseph, N.L., Waggoner, S.Z., Gulick, C.W., Korosec, M.A., and Bunning, B.B., 1991, Geologic map of Washington-Northeast quadrant: Washington Division of Geology and Earth Resources Geologic Map GM-39, 44 p.

Suydam, J.D., and Gaylord, D.R., 1997, Toroda Creek half graben, northeast Washington: Late-stage sedimentary infilling of a synextensional basin: Geological Society of America Bulletin, v. 109, p. 1333–1348, https://doi.org/10.1130/0016-7606(1997)109<1333:TCHGNW>2.3.CO;2.

Tabor, R.W., Engels, J.C., and Staatz, M.H., 1968, Quartz diorite-quartz monzonite and granite plutons of the Pasayten River area, Washington—Petrology, age, and emplacement: U.S. Geological Survey Professional Paper 600-C, p. C45–C52.

Tabor, R.W., Waitt, R.B., Jr., Frizzell, V.A., Jr., Swanson, D.A., Byerly, G.R., and Bentley, R.D., 1982, Geologic map of the Wenatchee quadrangle, Washington: U.S. Geological Survey Miscellaneous Investigations Map MI-1311, scale 1:100,000, 1 sheet, 31 p. text.

Tabor, R.W., Frizzell, V.A., Jr., Vance, J.A., and Naeser, C.W., 1984, Ages and stratigraphy of lower and middle Tertiary sedimentary and volcanic rocks of the Central Cascades, Washington: Applications to the tectonic history of the Straight Creek fault: Geological Society of America Bulletin, v. 95, p. 26–44, https://doi.org/10.1130/0016-7606(1984)95<26:AASOLA>2.0.CO;2.

Tabor, R.W., Frizzell, V.A., Jr., Whetten, J.T., Waitt, R.B., Swanson, D.A., Byerly, G.R., Booth, D.B., Hetherington, M.J., and Zartman, R.E., 1987, Geologic map of the Chelan 30-minute by 60-minute quadrangle, Washington: U.S. Geological Survey Geologic Investigation Series, I-1661, scale 1:100,000, 1 sheet, 56 p. text.

Tabor, R.W., Haugerud, R.A., and Miller, R.B., 1989, Overview of the geology of the North Cascades, in International Geological Congress Trip T307 Guidebook: Washington, D.C., American Geophysical Union, 62 p.

Tabor, R.W., Frizzell, V.A., Jr., Booth, D.B., and Waitt, R.B., 2000, Geologic map of the Snoqualmie Pass 30×60 minute quadrangle, Washington: U.S. Geological Survey Geologic Investigations Map MI-2538, scale 1:100,000, 1 sheet, 57 p. text.

Tabor, R.W., Haugerud, R.A., Hildreth, W., and Brown, E.H., 2003, Geologic map of the Mount Baker 30- by 60-minute quadrangle, Washington: U.S. Geological Survey Geologic Investigation Series I-2660, scale 1:100,000, 1 sheet, 70 p. text.

Tepper, J.H., 2016, Eocene breakoff and rollback of the Farallon slab—An explanation for the "Challis event"?: Geological Society of America, Abstracts with Programs, v. 48, no.4, paper 327-1, https://doi.org/10.1130/abs/2016CD-274512.

Tepper, J.H., Nelson, B.K., Clark, K., and Barnes, R.P., 2008, Heterogeneity in mantle sources for Eocene basalts in Washington: Trace element and Sr-Nd isotopic evidence from the Crescent and Teanaway basalts: Abstract V41D-2121, presented at 2008 Fall Meeting, American Geophysical Union, San Francisco, California, 15–19 December.

Thorkelson, D.J., 1996, Subduction of diverging plates and the principles of slab window formation: Tectonophysics, v. 255, p. 47–63, https://doi.org/10.1016/0040-1951(95)00106-9.

Thorkelson, D.J., and Taylor, R.P., 1989, Cordilleran slab windows: Geology, v. 17, p. 833–836, https://doi.org/10.1130/0091-7613(1989)017<0833:CSW>2.3.CO;2.

Tikoff, B., and Teyssier, C., 1994, Strain modeling of displacement-field partitioning in transpressional orogens: Journal of Structural Geology, v. 16, p. 1575–1588, https://doi.org/10.1016/0191-8141(94)90034-5.

Umhoefer, P.J., and Miller, R.B., 1996, Mid-Cretaceous thrusting in the southern Coast Belt, British Columbia and Washington, after strike-slip fault reconstruction: Tectonics, v. 15, p. 545–565, https://doi.org/10.1029/95TC03498.

Vance, J.A., and Miller, R.B., 1983, Geologic constraints on the movement history of the Straight Creek fault, in Yount, J.C., ed., Proceedings of Workshop XIV; Earthquake Hazards of the Puget Sound Region, Washington: U.S. Geological Survey Open-File Report 83–19, p. 302–306.

Vermeesch, P., 2018, IsoplotR: A free and open toolbox for geochronology: Geoscience Frontiers, v. 9, p. 1479–1493, https://doi.org/10.1016/j.gsf.2018.04.001.

Vigneresse, J.-L., Tikoff, B., and Ameglio, L., 1999, Modification of the regional stress field by magma intrusion and formation of tabular granitic plutons: Tectonophysics, v. 302, p. 203–224, https://doi.org/10.1016/S0040-1951(98)00285-6.

Wadge, G., Biggs, J., Lloyd, R., and Kendall, J.-M., 2016, Historical volcanism and the state of stress in the East African Rift System: Frontiers of Earth Science, v. 4, p. 86, https://doi.org/10.3389/feart.2016.00086.

Wallace, L.M., Beevan, J., McCaffrey, R., and Darby, D., 2004, Subduction zone coupling and tectonic block rotations in the North Island, New Zealand: Journal of Geophysical Research: Solid Earth, v. 109, https://doi.org/10.1029/2004JB003241.

Waters, A., 1927, Concerning the differentiation of lamprophyric magma at Corbaley Canyon, Washington: The Journal of Geology, v. 35, p. 158–170, https://doi.org/10.1086/623395.

Wells, R., Bukry, D., Friedman, R., Pyle, D., Duncan, R., Haeussler, P., and Wooden, J., 2014, Geologic history of Siletzia, a large igneous province in the Oregon and Washington Coast Range: Correlation to the geomagnetic polarity time scale and implications for a long-lived Yellowstone hotspot: Geosphere, v. 10, p. 692–719, https://doi.org/10.1130/GES01018.1.

Wells, R., Blakely, R.J., and Bemis, S., 2020, Northward migration of the Oregon forearc on the Gales Creek fault: Geosphere, v. 16, p. 660–684, https://doi.org/10.1130/GES02177.1.

Wells, R.E., Engebretson, D.C., Snavely, P.D., and Coe, R.S., 1984, Cenozoic plate motions and the volcano-tectonic evolution of western Oregon and Washington: Tectonics, v. 3, p. 275–294, https://doi.org/10.1029/TC003i002p00275.

Wernicke, B.P., and Getty, S.R., 1997, Intracrustal subduction and gravity currents in the deep crust; Sm-Nd, Ar-Ar, and thermobarometric constraints from the Skagit Gneiss Complex, Washington: Geological Society of America Bulletin, v. 109, p. 1149–1166, https://doi.org/10.1130/0016-7606(1997)109<1149:ISAGCI>2.3.CO;2.

Wintzer, N.E., 2012, Deformational episodes recorded in the Skagit Gneiss Complex, North Cascades, Washington, USA: Journal of Structural Geology, v. 42, p. 127–139, https://doi.org/10.1016/j.jsg.2012.06.004.

Wolf, M.B., and Saleeby, J.B., 1992, Jurassic Cordilleran dike swarm–shear zones: Implications for the Nevadan orogeny and North American plate motion: Geology, v. 20, p. 745–748, https://doi.org/10.1130/0091-7613(1992)020<0745:JCDSSZ>2.3.CO;2.

Zoback, M.L., and Zoback, M., 1980, State of stress in the conterminous United States: Journal of Geophysical Research: Solid Earth, v. 85, p. 6113–6156, https://doi.org/10.1029/JB085iB11p06113.